(2)

THE FEASIBILITY OF EVENT SEQUENCE DISCRIMINATION FOR THE IMPROVEMENT OF GAMMA-RAY SPECTROMETER SENSITIVITY

Final Report

Contract No. DASG60-89-C-0083

by

D. M. Walker, Principal Investigator
B. G. Wahlig
J. H. Gillespie

SPONSORED BY
SDIO Innovative Science and Technology Office

MANAGED BY
U.S. Army Strategic Defense Command

December 29, 1989

QUANTUM TECHNOLOGY, INC.
830 Franklin Court
Marietta, Georgia 30067

SECURITY CLASSIFICATION OF THIS PAGE

REPORT DOCUMENTATION PAGE

Form Approved OMB No. 0704-0188

1a. REPORT SECURITY CLASSIFICATION Unclassified	1b. RESTRICTIVE MARKINGS N/A
2a. SECURITY CLASSIFICATION AUTHORITY N/A	3. DISTRIBUTION/AVAILABILITY OF REPORT Unrestricted
2b. DECLASSIFICATION/DOWNGRADING SCHEDULE N/A	
4. PERFORMING ORGANIZATION REPORT NUMBER(S) DASG60-89-C-0083	5. MONITORING ORGANIZATION REPORT NUMBER(S)
6a. NAME OF PERFORMING ORGANIZATION Quantum Technology, Inc.	6b. OFFICE SYMBOL (If applicable) N/A
6c. ADDRESS (City, State, and ZIP Code) 830 Franklin Court Marietta, GA 30057	7a. NAME OF MONITORING ORGANIZATION 7b. ADDRESS (City, State, and ZIP Code)
8a. NAME OF FUNDING/SPONSORING ORGANIZATION USAMICOM/AMSMI-RM-FA-AA-CS	8b. OFFICE SYMBOL (If applicable)
8c. ADDRESS (City, State, and ZIP Code) Finance and Accounting Office, Bldg. 8027 Redstone Arsenal, AL 35898-5092	9. PROCUREMENT INSTRUMENT IDENTIFICATION NUMBER DASG60-89-C-0083
	10. SOURCE OF FUNDING NUMBERS PROGRAM ELEMENT NO. KE-9 / PROJECT NO. / TASK NO. / WORK UNIT ACCESSION NO.

11. TITLE (Include Security Classification)
The Feasibility of Event Sequence Discrimination for the Improvement of Gamma-Ray Spectrometer Sensitivity

12. PERSONAL AUTHOR(S)
Walker, David M.; Wahlig, Barry G.; Gillespie, Jim G.

13a. TYPE OF REPORT	13b. TIME COVERED	14. DATE OF REPORT (Year, Month, Day)	15. PAGE COUNT
FINAL	FROM 89/5 TO 89/11	89/12/29	112

16. SUPPLEMENTARY NOTATION

17. COSATI CODES		
FIELD	GROUP	SUB-GROUP
18	04	
06	18	

18. SUBJECT TERMS (Continue on reverse if necessary and identify by block number)
Semiconductor Radiation Detectors; Gamma-Ray Spectrometer; Radiation Monitoring; (AW)

19. ABSTRACT (Continue on reverse if necessary and identify by block number)

Nuclear measurement applications for military surveillance, environmental monitoring, and physics research are bounded by detection sensitivity and counting time limitations. To date, improvements in detection sensitivity for semiconductor detectors have been limited to small incremental gains made primarily through increased crystal size and purity. The results of this study indicate that a step improvement in the gamma ray detection sensitivity of semiconductor detectors is achievable if information on each scattering sequence can be processed and used on a livetime basis to accept preferentially the full energy event sequences, and to reject "false" partial energy event sequences.

In this study, a Monte Carlo model for gamma ray interactions in germanium was developed and used to select criteria on interaction location and number of events which are predicted to improve detector performance. The sensitivity of a detector system was determined from the Monte Carlo model results for five gamma ray energies in the range 88 keV to 1836 keV, under several event discrimination criteria. The predicted (See Back)

20. DISTRIBUTION/AVAILABILITY OF ABSTRACT	21. ABSTRACT SECURITY CLASSIFICATION
☒ UNCLASSIFIED/UNLIMITED ☐ SAME AS RPT. ☐ DTIC USERS	Unclassified

22a. NAME OF RESPONSIBLE INDIVIDUAL	22b. TELEPHONE (Include Area Code)	22c. OFFICE SYMBOL
Dr. David Lukins, Physical Scientist	(205) 895-5017	CSSD-H-V

DD Form 1473, JUN 86 Previous editions are obsolete. SECURITY CLASSIFICATION OF THIS PAGE

19. counting time required to achieve a given detection sensitivity was found to be reduced by 14% to 64%, compared tc conventional detector systems, for the most successful event sequence processing mode.

The event sequence discrimination modes that were modeled mathematically now appear to be practicably achievable through detector segmentation and/or pulse rise time analysis. In addition, physical mechanisms and measurement methods were indentified which may allow (after further research) for achieving the ideal in event discrimination: distinguishing between sequences ending in photoelectric and Compton interactions.

QUANTUM TECHNOLOGY CONTRACT DASF60-89-C-0083

ADVANCED CONCEPT FOR GAMMA RAY DETECTORS

Special Technical Summary

(a) Procuring Activity Designated Order Number: CARN 9C1461

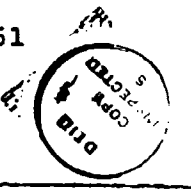

Accesion For	
NTIS CRA&I	☑
DTIC TAB	☐
Unannounced	☐
Justification	
By	
Distribution/	
Availability Codes	
Dist	Avail and/or Special
A-1	

(b) Name of Contractor: Quantum Technology
830 Franklin Court
Marietta, GA 30067

(c) Contract Number: DASG60-89-C-0083

(d) Effective Date of Contract: 26 May 89

(e) Expiration Date of Contract: 25 Nov 89

(f) Reporting Period: Final Report

(g) Principal Investigator and Phone No.: Dr. David M. Walker (404) 429-8324

(h) Project Scientist or Engineer and Phone No.: Dr. David M. Walker (404) 429-8324

(i) Short Title of Work: Advanced Concept for Gamma Ray Detectors

NOTICE: The views and conclusions contained in this document are those of the authors, and should not be interpreted as necessarily representing the official policies, either expressed or implied, of the Government.

SPONSORED BY
SDIO Innovative Science and Technology Office

MANAGED BY
U.S. Army Strategic Defense Command

TABLE OF CONTENTS

TABLE OF CONTENTS (continued)

LIST OF TABLES

LIST OF FIGURES

LIST OF FIGURES (continued)

EXECUTIVE SUMMARY

Semiconductor detectors are a most powerful tool for characterizing gamma emissions from an unknown source, and for quantitative analysis of mixed radionuclides in a sample. Since the development of semiconductor detectors in the mid 1960's, gamma ray spectroscopy has become an indispensable part of physics research, and of nuclear process and environmental monitoring. The small size and weight of semiconductor detectors and their related processing electronics has spawned a number of important space research projects and military surveillance applications based on gamma ray analysis.

Because of the variety of beneficial applications of gamma spectroscopy, an ongoing effort for improved semiconductor detector performance has produced a steady stream of advancements over the past 25 years. These advancements are primarily due to the development of larger, higher purity crystals, and to the application of passive and active shielding systems. Improvements in performance from these approaches have now reached a point of sharply diminishing returns.

This study explored an alternate approach of processing and analyzing the output from a semiconductor detector which, if successful, would represent a departure from the evolutionary advancements now being realized in the field. The "event sequence analysis" approach involves processing information from the gamma ray interaction sequence in a detector, not as a single event, but as an interaction sequence whose nature could be used to preferentially accept full energy pulses, and to reject partial energy sequences.

Conventional detector systems simply collect the sum of the electron-hole charge in the detector from all gamma ray interactions in an event sequence, and indicate only that an event has occurred which corresponds to the absorption of a certain amount of gamma ray energy within the detector. In the event sequence analysis approach, parameters such as the number of interactions in the event sequence, the location of the interactions, and the energy deposition pattern are measured and compared to prescribed criteria to determine if the event is to be accepted or rejected.

The first steps in this study were to develop a Monte Carlo model which would accurately describe gamma interaction behavior in a semiconductor detector, and to use the model to identify patterns in the interaction sequence which could be used to preferentially accept full energy events. The Monte Carlo model was then operated with parameters of a hypothetical detector to predict performance. Various event sequence criteria were imposed to determine if improved performance was likely in an actual detector over an energy range of interest.

A second concurrent step of the study was a search of related literature to determine if practical means of implementing the event sequence criteria on an operating detector could be identified. In order to assure that ample previous research and experimental performance information would be available to corroborate the Monte Carlo analyses, the Phase I study was limited to intrinsic germanium photon detectors.

Monte Carlo calculations were performed for selected incident gamma ray energies and were used to generate tabular and graphical listings of gamma scattering results. The tabular listings gave descriptions of individual interactions within the detector (interaction number, location, and energy deposition) and of the resulting "spectrum." Graphical presentations of the event location, number distribution, and spectrum for any set of prescribed conditions were also generated. These output presentations were studied to identify behavior patterns of "good" and "bad" event sequences.

For the specific gamma energy range and detector geometry selected for this study, the results of the Monte Carlo calculations suggested that for analyzing low energy gamma rays in the presence of higher energy interference, the acceptance of single interaction events within the top 5 mm would provide improved performance. The data also indicated that for gamma incident energies above 100 keV the average number of interactions in a "good" event sequence was much greater than one, while one-interaction events always dominated the Compton escape process.

For a hypothetical coaxial detector of 6 cm diameter and 8 cm length, Monte Carlo runs were made with various event sequence criteria imposed on the output. A figure-of-merit index including both peak energy efficiency and background was used to compare detector performance to assure that overall sensitivity, rather than just background suppression, was being compared. For the incident gamma ray energies examined (88, 320, 661, 1115, and 1836 keV), individual event sequence criteria were identified which gave sensitivity figure-of-merit improvements ranging from 18% to 182%, or decreases in counting time for equivalent sensitivities of 14% to 64%. These improvements are significant when compared to improvements expected from advances in conventional techniques for the foreseeable future.

During the Phase I effort, studies of reported research in semiconductor detectors identified several promising methods to determine the position of interactions in a detector, and the occurrence of multiple interaction event sequences. Both theoretical and experimental performance of segmented detectors indicates that this technique should allow identification of the location of gamma ray interactions. Reported studies of rise time rate for charge collection indicates that analysis of the pulse rise time would provide position information, and an indication of multiple interaction events.

One event sequence criterion stands out as the ultimate Compton background suppression technique: the ability to distinguish between event sequences ending in a Compton or in a photoelectric interaction. A cursory study of this possibility showed that physically distinct interaction and de-excitation processes accompany Compton and photoelectric interactions, and that the primary product of each is a dense electron-hole plasma in the lattice.

Independent research into spontaneous and stimulated oscillations in germanium by various research groups over the past ten years has characterized several oscillatory phenomena related to electron-hole plasmas and subsequent impact ionization. It is possible, although by no means certain, that an oscillatory phenomenon related to the dense electron-hole plasma created by gamma interactions in germanium could be characterized external to the detector by analyzing the AC or optical outputs related to the process. This area is recognized as speculative, but of high return, and could be pursued on a limited basis by empirical testing using the processing circuitry which will be required for applying the more conventional rise time analysis technique.

Several conclusions can be drawn from the Phase I study. First, the use of event sequence techniques does appear to give useable sensitivity and counting time improvements for specific measurement applications. Secondly, practical techniques exist to implement event sequence analysis in semiconductor detector counting systems based on recent advances in detector fabrication and in small low power analog and digital electronics circuitry.

Event sequence analysis techniques appear to address several important requirements for military and space applications. Counting systems based on this technique can be small: they combine knowledge of the scattering process with capabilities offered by recent developments in low power analog and digital microcircuitry to gain performance improvements with minimal weight and size penalties. In some cases, the performance offered in terms of improved sensitivity and reduced counting time simply cannot be achieved by conventional detector or shielding technology.

Although this advanced detector technology is being developed primarily for military application, the benefits to nuclear process and environmental monitoring, as well as to general laboratory gamma spectroscopy, are obvious. In fact, it is a rare gamma spectroscopy application which would not benefit from improved sensitivity and reduced counting time.

A Phase II effort to develop methods for implementing and verifying the performance of event sequence analysis techniques will be proposed.

1. BASIS FOR EVENT SEQUENCE DETECTORS

1.1. Status of Conventional Technology

The objective of this research is to determine if event sequence analysis methods potentially offer significant performance improvements in detection sensitivities for high-resolution gamma ray spectroscopy. In order to appreciate the need for this work, one must first have some knowledge of the current state of the art in this area, and of the capabilities and limitations of current methods for improved system performance. This section presents the required background.

Although the focus of the Phase I study was confined to germanium detectors, the concepts discussed would generally be applicable to other elemental or compound semiconductor detectors. Germanium detectors were chosen for this study because of the extensive research base which is well documented in the literature, and because of the broad applicability of improved germanium detector performance to both space and conventional applications.

1.1.1. Description of Current Semiconductor Gamma Ray Spectrometers

In the late 1980's, all new laboratory high-resolution gamma ray spectrometers for routine sample assay are essentially identical in design and operation. The block diagram of a typical system is shown in Figure 1-1, and is discussed below.

The detector is a bulk diode of high-purity elemental germanium (HPGe), operated at a high reverse bias. HPGe detector crystals are cylindrical, and are usually manufactured in a planar geometry or in one of the three coaxial geometries shown in Figure 1-2. Planar detectors, with electrical contacts only on the two flat faces of the cylinder, are preferred for high count rate and low energy applications. The advantage of the coaxial geometry is that, when reverse-biased, it develops a charge-depleted region of larger volume for the same applied high voltage than does the planar geometry. Coaxial detectors are generally about 5 to 8 cm in diameter, and roughly the same or slightly larger dimension in height. Only a few tens of volts are required to produce full charge depletion in such a crystal, but its practical operating voltage will be on the order of 5000 volts; this ensures maximum collection of the charge carriers generated by the interactions of gamma rays in the compensated region.

Figure 1-1. Standard High-Resolution
Gamma Ray Spectrometer System

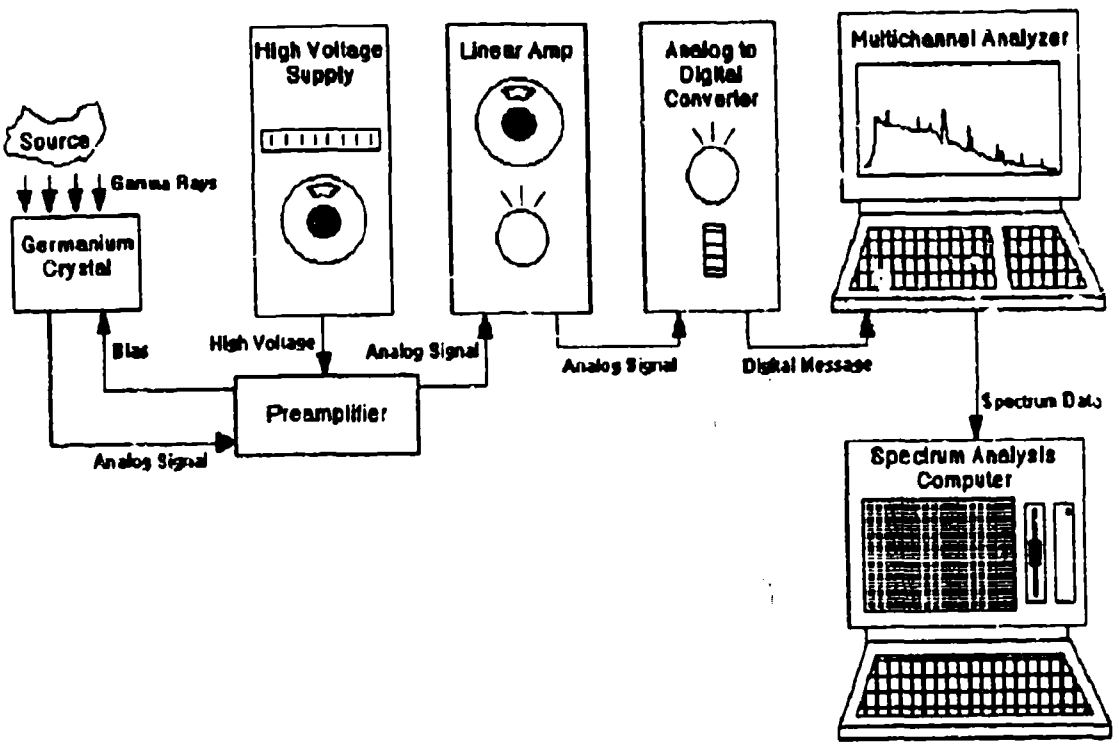

Figure 1-2. Cross-Sections of Germanium Detector Geometries

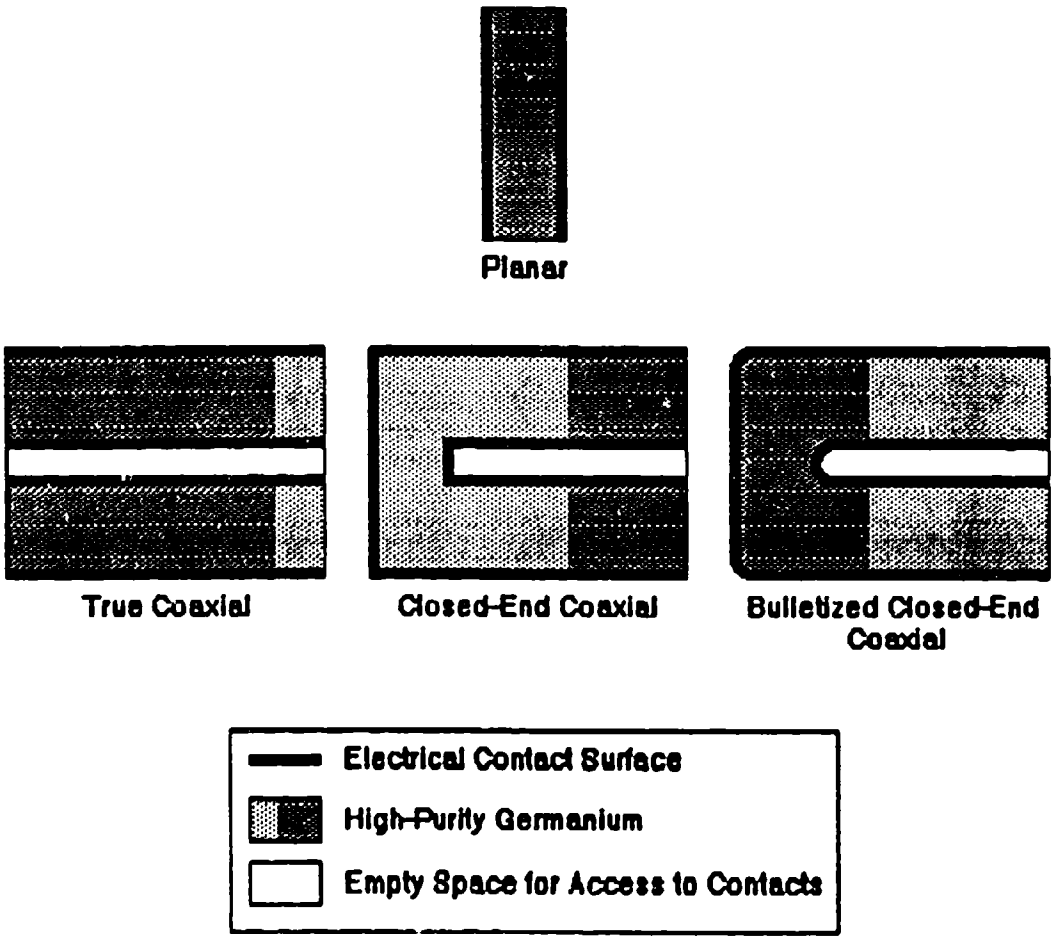

As depicted in Figure 1-1, the charge pulses produced in the detector by the absorption of gamma radiation energy are amplified and processed in external circuitry. The resulting voltage pulses are sorted by pulse size into a large number of incremental "channels" (typically 4096) by an analog-to-digital converter. The digitized information is counted and displayed by the multichannel analyzer (MCA). After data acquisition is complete, the digital data which makes up the pulse height spectrum are normally analyzed by specialized application software on an external computer.

An example gamma ray pulse height spectrum from a standard system is shown in Figure 1-3. In such a spectrum, only certain of the peaks (the Full Energy Peaks) contain useful information: it is only the channel location of each peak which can be correlated with gamma ray energy (and therefore with responsible radionuclide); and it is only the net area of the peak which can be correlated with gamma ray emission rate (and therefore with sample activity).

Everything else in the spectrum represents noise and interference, as far as the assay process is concerned. In particular, the majority of the recorded counts form the baseline continuum under the peaks: this continuum contains no useful information, and serves to set an uncertainty limit on the ability to quantify data in the full energy peaks.

1.1.2. General Performance Criteria for Gamma Ray Spectrometers

Many parameters can be used to gauge and monitor the performance of gamma ray spectrometers. However, for the purposes of this report, the desirable operational parameters are the following:

1. High Efficiency. In a high-efficiency detector, a large fraction of the gamma rays emitted by the source finally result in counts in the full energy peaks of the collected spectrum. In general, the larger the detector, the more of the gamma rays entering the detector will convert their full energy into charge carriers within the active detector volume. The evolutionary improvement in gamma spectrometer efficiency that has occurred to date is the result of improvements in the manufacturing processes, permitting the growth of larger germanium crystals of acceptable purity and structural perfection.

Figure 1-3. Pulse Height Spectrum from a Standard Germanium Gamma Ray Spectrometer

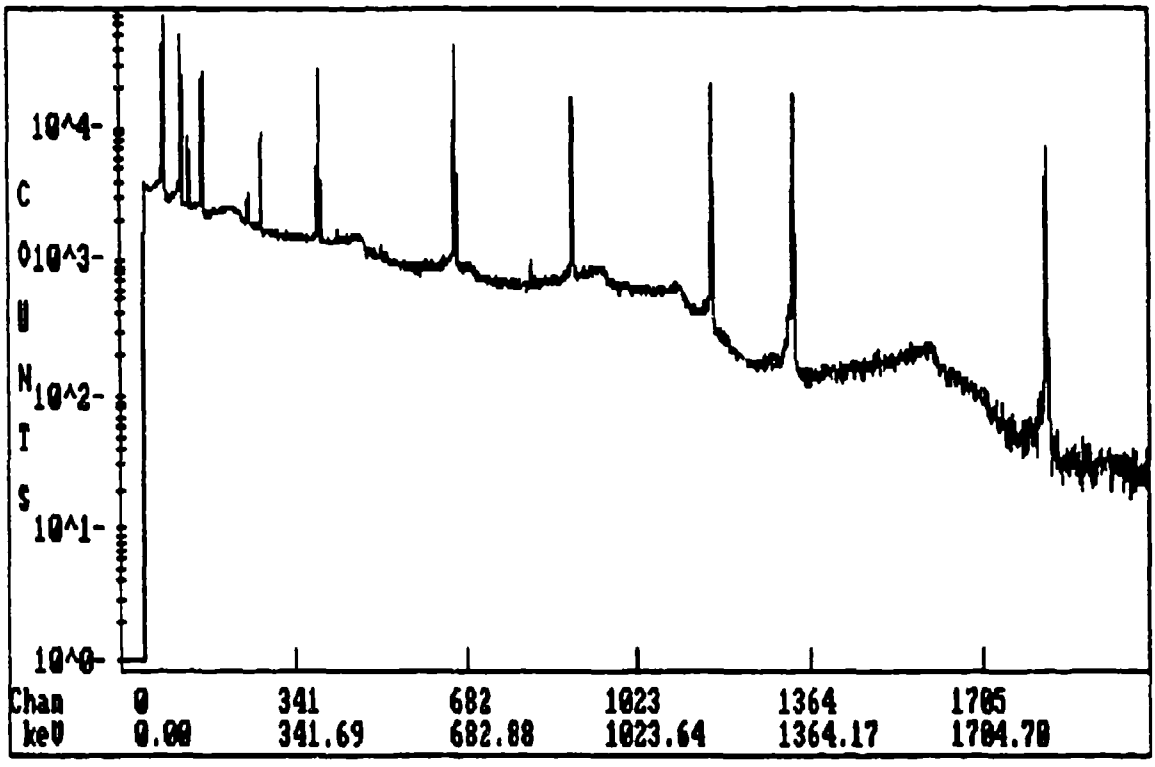

2. High Resolution. High resolution in a detector system provides improved ability to distinguish between gamma rays of roughly the same energies. In the example of Figure 1-3, resolution relates to the observed widths of the peaks: detectors with the best resolution have the narrowest peaks, which permits improved quantitative separation of closely spaced peaks.

   High resolution requires complete, uniform charge collection and low electronic noise in the pulse processing circuitry. Further improvements in resolution are expected to be evolutionary, barring a new generation of lower-noise preamplifiers.

   Note that larger coaxial crystals have somewhat greater variability in charge collection (and worse resolution) because of the greater variation in electric field across their depleted region. Therefore, using larger crystals to improve efficiency conflicts, above a certain detector size, with the desire to improve resolution.

3. Low Background. The background of a gamma spectrometer at a given energy is the sum of all recorded counts at that energy which are produced by any interaction sequence other than the absorption of the total energy of the incident gamma ray of interest. In gamma spectroscopy, the background at a given energy consists primarily of three components: (a) the continuum of counts produced by the interactions of cosmic rays in the detector and the surrounding materials; (b) the characteristic peaks and Compton continuum produced by gamma rays emitted by radioactive materials (whether natural or manmade) located outside the sample; and (c) the Compton continuum produced by the partial absorption in the detector of higher-energy gamma rays emitted by radioactive materials in the sample.

   Of these three contributions, only the first two are subject to improvement by the use of bulk passive shielding around the detector and sample. The Compton continuum due to higher-energy gamma rays from the source of interest can only be suppressed by active electronic means.

   All three of the background contributions are random, and are governed by Poisson statistics; therefore, the background continuum (despite its general downward trend with increasing energy) is not a smooth and monotonic function of energy. Each of the three background components will exhibit channel-by-channel fluctuations as governed by Poisson statistics, and will contribute in the same manner to the uncertainty in quantifying a

superimposed full energy peak. Additional information on the methods used to date for background reduction is presented in Section 1.1.4.

4. Sensitivity. A measure of the sensitivity of a gamma spectrometer is its ability to distinguish low-count rate pulses resulting from one radionuclide in the presence of pulses of about the same pulse height produced by background events. Since detection of low levels of radionuclides in the presence of interference is the most difficult test of a spectrometer, numerical values of sensitivity are probably the most useful parameters in judging the quality of a system.

   Regardless of the exact measure used for sensitivity (lower limit of detection, critical level, minimum detectable concentration, etc.), the most sensitive system is one which has a low value for the expression: $(\sqrt{B})/\epsilon$. That is, the most sensitive spectrometer will, at a given energy, have a high full energy peak efficiency ϵ, and low background B (Cu84). This means that raising efficiency alone does not necessarily give an improvement in sensitivity, if it comes at the cost of too great an increase in background; nor is a decrease in background necessarily a good thing, if it is achieved by lowering the system's detection efficiency. This important consideration must not be overlooked in pursuing background reduction techniques.

1.1.3. Special Criteria for Space-Based Spectrometer Systems

The performance criteria discussed in Section 1.1.2 are applicable to any gamma ray spectrometer, regardless of its purpose. In addition, certain other considerations are applicable to mobile installations in general, and to space-based installations in particular.

1. Light Weight. Every few grams saved in orbital payload weight results in appreciable fuel savings for a space mission. Therefore, spectrometer systems which achieve adequate performance without resort to heavy and bulky shielding are strongly preferred.

2. Flexibility of Application. Related to weight is flexibility. If the spectrometer system is designed so that it can be configured to serve multiple purposes in space, it may obviate the need to lift one or more additional systems in the payload.

3. Ruggedness. The buffeting accelerations of liftoff are well known. They argue strongly in favor of solid state electronic devices, and against any systems based on vacuum tubes or complex mechanical arrangements.

1.1.4. Prior Approaches to Improving Gamma Ray Spectrometer Sensitivity

Section 1.1.2 stated that sensitivity is the most demanding test of the performance of gamma ray spectrometers. Therefore, the following brief listing of improvements which have been made in the basic spectrometer design concentrates on those which have a beneficial effect on sensitivity.

1. Larger Detectors. There has been a steady increase in the maximum size of detector crystal commercially obtainable. Today, detectors with sensitive volumes greater than 100 cm^3 are stock items.

   In general, larger crystal size provides better efficiency, and therefore better sensitivity. However, above a certain crystal size, the sensitivity gains decrease because of preferential gains in efficiency for background components, and because of loss of resolution due to poorer charge collection.

   In practice, the price/performance curve is now very steeply sloped for the largest detectors. Only a small number of the largest crystals can be grown successfully, and the diminishing performance returns ensure that the price per unit of efficiency rises sharply as the limit of current commercial production capability is approached. Performance improvements of only a few percent per year as result of increased crystal size can be expected over the next few years.

2. Passive Shielding. Passive shielding consists of surrounding the detector with inert materials for the absorption of non-sample radiation. The type, sequence, and thickness of the materials determine which radiation(s) are shielded, and to what extent. The selection of sources of materials may be as significant as the choice of the types and thicknesses, since sources of materials vary considerably in the amounts of natural and manmade radionuclides that they contain (Ma84, Re84, Re85).

   A simple shield of lead or iron will attenuate gamma rays, but may bathe the detector in an undesirable flux of characteristic X-rays resulting from the interactions of radiation in the shield metal. The X-rays may be eliminated by adding to the inside of the shield a series

of lower-atomic-number metal layers (such as tin, then copper). If cosmic-ray-induced activity is a significant concern, the shield may include a layer of metal, followed by low atomic-number material (such as water, to thermalize neutrons), and a layer of cadmium (to absorb the thermalized neutrons).

The greatest disadvantages of passive shielding are mass and bulk, since in order to be effective, they must be thick and heavy. A typical general-purpose germanium spectrometer shield is about 10 cm thick, and weighs about 1.2 tonnes; a shield which includes anti-neutron layers may be 25-30 cm thick and weigh more than 2.5 tonnes. Such shielding has obvious limitations in any mobile or space application. In addition to the weight and bulk drawbacks, it must be noted that passive shields reduce only two of the three components of spectrometer background, leaving the Compton continuum from in-sample interferences unaffected.

3. Active Shielding. The principle of active shielding is to surround the sample detector with other radiation detectors which are operated in anti-coincidence with the sample detector. Thus, although the shield detectors do not prevent the occurrence of background events in the sample detector, they can recognize the occurrence of coincident events and cause their rejection.

Most commonly, the shield detectors are intended to detect and reject events in which a gamma ray from the sample is only partially absorbed in the sample detector. Without coincidence rejection, this type of event would lead to a count in the Compton continuum of the sample spectrum, so shield detectors operated in this way are also called Compton Suppression Spectrometers. They are usually constructed from a solid scintillator such as sodium iodide or bismuth germanate, and achieve reduction factors in the continuum counts per channel on the order of 3 to 10 (Al88, Mi86, Ve86).

Compton Suppression Spectrometers also have some effect on non-sample background counts. However, when non-sample background is the primary concern, the active shield is often in the form of a layer of plastic or liquid scintillator outside the primary gamma shield (see, for example: Re84, Re85). An active shield of this type will detect not only photons (although at rather low efficiency), but also neutrons and charged particles which may interact in the gamma shield to produce photons. Such a system will reduce non-sample background counts per channel by a factor of 10 to 50,

but will not suppress the Compton continuum significantly.

Despite their successes, active shields can have appreciable disadvantages in terms of size, weight, and lack of ruggedness. The active shield may itself be heavy, as in the case of thick scintillator located outside the gamma shield; but when a Compton Suppression Spectrometer must be located inside the passive gamma shield, the passive shield's internal cavity must be made larger, and its weight rises cubically.

A second disadvantage is that the active shield (especially a Compton Suppression Spectrometer) must be near the sample detector. As a result it often restricts access to the detector, and may limit the size and shape of samples that can be mounted.

Finally, active shields are not well suited to mobile applications because they use scintillator detectors, and often multiple scintillators. This not only introduces the problems of coincidence timing and gain matching between the detectors, but it also inserts delicate photomultipliers (which are vacuum tubes) into what would otherwise be a pure solid state system.

4. Segmented Detectors. A study of gamma ray interaction behavior shows that, for a given amount of energy deposited in a detector, event sequences in which the total energy is captured usually involve more interactions than do event sequences ending in the escape of a Compton scattered photon. Compton suppression spectrometers using this phenomenon have been produced by operating two or more independent germanium detector regions in the sum-coincidence mode. Thus, the sum of the charge from all regions is accepted as an event only if gamma interactions are simultaneously observed in two or more independent detector regions.

Two-region Ge(Li) and HPGe detectors of this type have been built and tested, and achieved drastic continuum reductions (Pa68, Va84, Wa70b). However, because of the coarse spatial resolution of an detector divided along a diameter, the efficiency was also decreased and the overall improvement in sensitivity was marginal. Plans and Monte Carlo analyses for HPGe detectors with six or more thickness elements have been reported (Ge84, Va84); the developers of these detectors expect to achieve greater improvements in sensitivity by minimizing the efficiency penalty of segmentation.

1.2. Basis for Event Sequence Analysis

The present research concerns itself with a fundamental, rather than an evolutionary, change in gamma spectroscopy: the development of what may be called an event sequence analysis spectrometer. For the purposes of this study, event sequence analysis will be defined as a gamma spectroscopy method in which certain measured characteristics of each gamma interaction sequence within a single detector are used on a dynamic basis to accept or reject the event.

Note that the concept of rejecting "bad" events based on the event sequence is the basis for both active shielding and the segmented detectors discussed in previous subsections. In anti-coincidence active shield devices, the presence of an event in the shield detector indicates that the event sequence in the sample detector ended in a Compton or pair production event in the sample detector, and thus the event sequence can be rejected as not representing a full energy event. Segmented detectors use one aspect of event sequence analysis by imposing a single criterion that the event sequence have more than one interaction, thus favoring multiple scattering events which are more likely to be full energy events.

In moving from these specific cases to a general application of event sequence analysis, it is necessary to examine in more detail the interaction behavior leading to "good" and "bad" events. Figure 1-4 shows the gamma interaction probability in germanium as a function of gamma ray energy, and Figure 1-5 shows the Compton scattering angle distribution for various incident gamma ray energies.

From Figure 1-4, it is seen that for incident gamma rays in the nominal energy range of about 1 MeV, the probability for a Compton interaction on the first interaction is at least 50 times greater than for a photoelectric event. Each successive Compton scatter produces a secondary gamma ray of less energy, and the strong forward scattering pattern for higher energies becomes nearly isotropic as the gamma ray energy decreases (see Figure 1-5).

Thus, with each Compton scatter in a sequence, it becomes more likely that the Compton scattered gamma photon will be directed back into the detector. It is also more likely that a photo-electric interaction will occur with each step reduction in energy (step to the left on the interaction probability graph of Figure 1-4). The probability that the event sequence will end in a total energy absorption by photoelectric interaction therefore becomes very great if enough scattering interactions occur to reduce the photon energy to 100 keV or less.

Figure 1-4. Gamma Ray Linear Attenuation Coefficient of Germanium

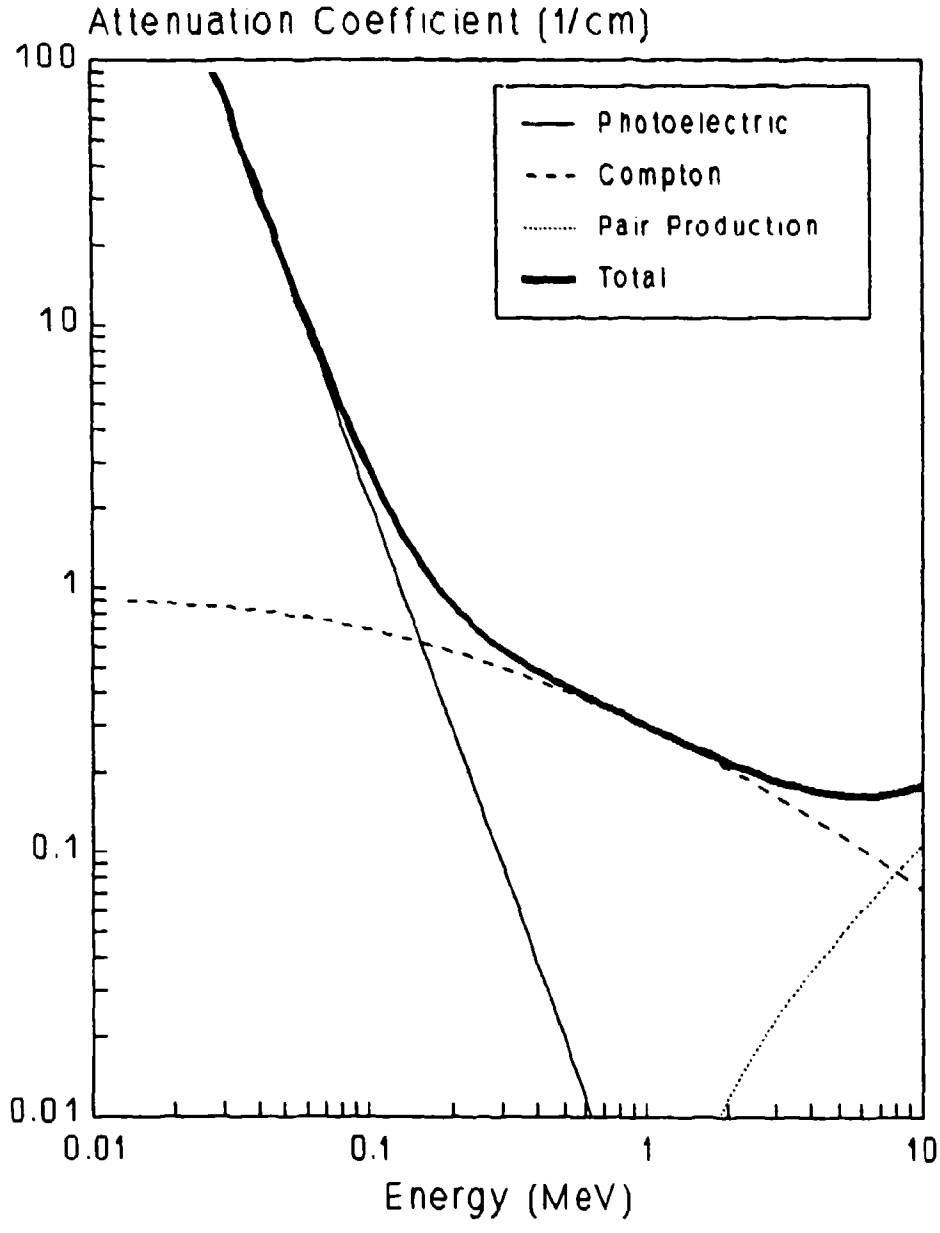

Figure 1-5. Angular Distribution of Compton Scattered Photons

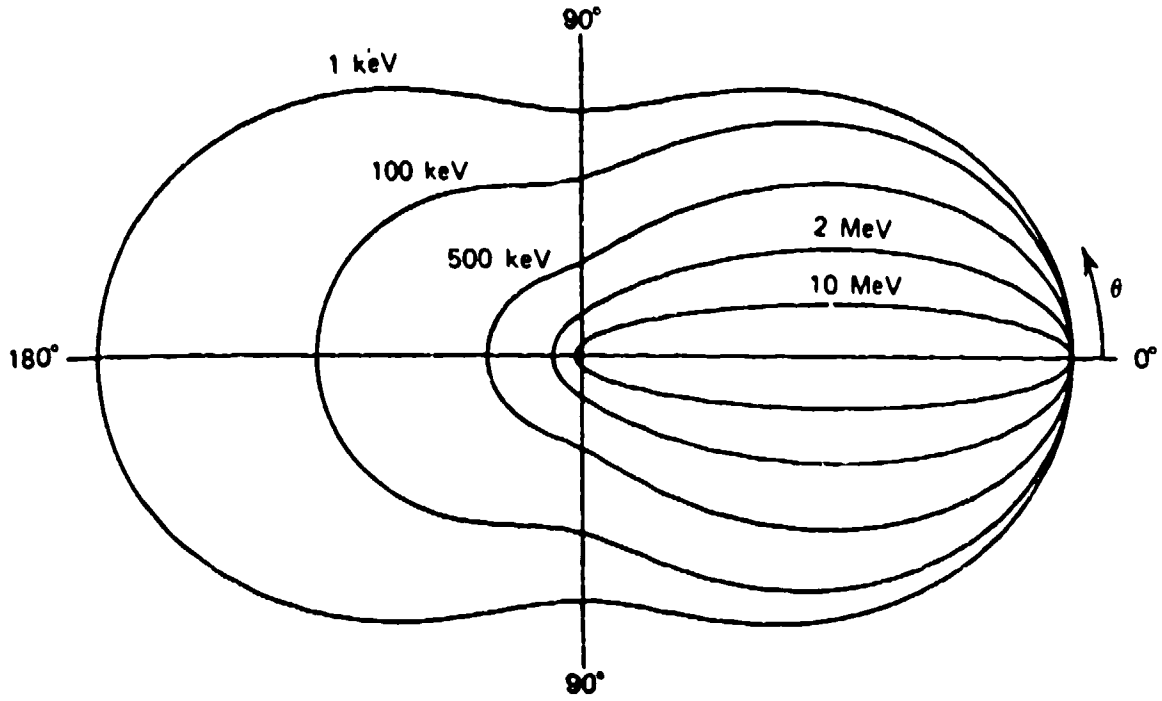

In contrast, an incident gamma ray of less than 100 keV in energy would, with high probability, be absorbed in a single photoelectric interaction. Since the interaction cross section becomes quite large for low energy photons, these single interactions are most likely to occur within a short distance of the front surface of the detector.

It is this kind of intuitive reasoning which suggests that detection sensitivities might be improved if some criterion such as the number, location, or energy release of interactions could be used to preferentially accept "good" event sequences ending in total energy capture, while rejecting "bad" events likely to end in the escape of photons from the detector. The Phase I effort sought to develop a methodical basis for determining criteria to be applied for specific detector applications, and for estimating the resulting performance.

Because of the difficulty of intuitively estimating detector performance resulting from imposing event sequence criteria on an operating semiconductor detector, it was necessary to either develop a reasonable computer model of the scattering phenomena, or to fabricate a number of detectors for experimental parameter studies. The computer modeling approach was selected for this Phase I effort as being both cost effective and more informative as to the actual nature of the interaction sequences for a range of gamma ray energies and detector geometries.

A Monte Carlo model was developed and used which cataloged each interaction as to type, location, and energy deposited. The basic interaction information was listed and graphed in several presentations which facilitated review and selection of promising event sequence criteria. Performance with any number of criteria could then be calculated for desired detector geometries and incident gamma ray energies and intensities. A brief description of the Monte Carlo model, and a discussion of the type of data presentations available from the model are given in Section 2. Appendix B provides a more detailed description of the basis and operation of the Monte Carlo model.

Reviews of the data in Section 2 as generated by runs with the Monte Carlo model were used to devise event sequence criteria which appeared to offer improved detection sensitivity. As discussed in Section 3, a few selected criteria for particular applications were evaluated by Monte Carlo computer runs for specified detector and source configurations. The calculated detector performance showed the difficulty of intuitive analysis, even with the general scattering information as a guide in selecting event sequence criteria: some of the selected criteria improved performance, while others degraded performance as compared to normal operation.

In order to use event sequence analysis, it is necessary to have practical means of observing characteristics of the sequence in an operating detector, of processing the information, and of applying the predetermined criteria on a live-time basis. In Section 4, several methods are identified which can provide livetime information on event location, number of events, and energy deposition within a detector. These methods would be used to implement event sequence analysis criteria in an operating gamma ray spectrometer.

Such a device, as shown conceptually in Figure 1-6, would resemble a standard gamma spectrometer in that it would sort the collected electronic pulses by size, and use the spectrum (along with the known characteristic emissions of radionuclides) to identify the radionuclides responsible for the spectrum.

It would differ from a standard spectrometer in that it would use an active discrimination technique to preferentially accept pulses resulting from event sequences in which the full energy of the incident gamma is deposited in the detector. Specifically, it would accept only those pulses which met a set of criteria that would substantially favor full-energy pulses over those that represent only partial deposition of the incident gamma energy.

In Section 5, the plausibility is examined of directly distinguishing an event sequence ending in a photoelectric absorption from a sequence ending in a Compton scattering interaction. All event sequence criteria are based indirectly on the fact that a "good" event sequence must end in a photoelectric absorption event within the detector, whether it occurs on the first interaction or on any subsequent interaction. Although an effort to directly determine event type is realized to be of higher risk, the step improvement in gamma ray spectrometry capability offered by progress in this area appears to justify limited further investigation.

Conclusions from the Phase I study are given in Section 6, and topics to be pursued in the Phase II effort are discussed in Section 7.

Figure 1-6. Conceptual Diagram of
Gamma Ray Event Sequence Discrimination Spectrometer

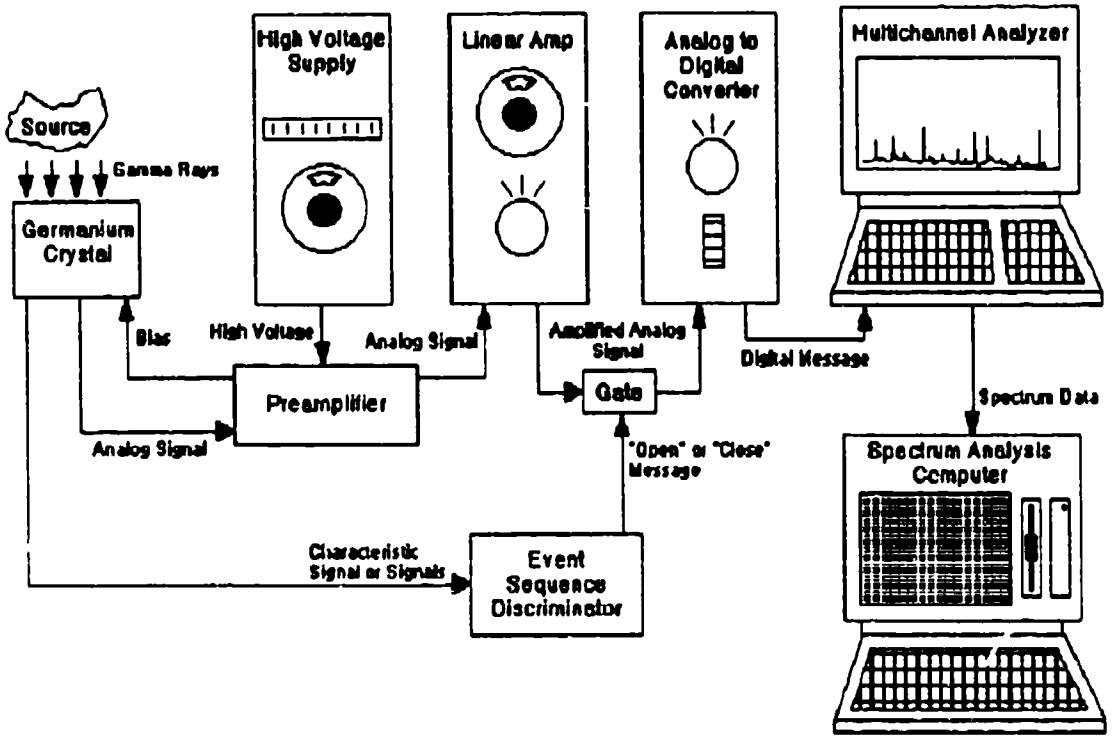

1.3. References

Al88 Alba, R.; Bellia, G.; Del Zoppo, A. "Performance of a Symmetric BGO-NaI Anti-Compton Shield." Nuc. Inst. and Meth. in Phys. Res. A271:553-556; 1988.

Cu84 Currie, L.A. "Lower Limit of Detection: Definition and Elaboration of a Proposed Position for Radiological Effluent and Environmental Measurements." USNRC Rept. NUREG/CR-4007; 1984.

Ev55 Evans, R.D. The Atomic Nucleus. New York:McGraw-Hill Book Co.; 1955.

Ge84 Gehrels, N.; Cline, T.L.; Teegarden, B.J.; Tueller, J.; Leventhal, M.; MacCallum, C.J.; Hewka, P.V.; Ryge, P. "The Development of a Segmented N-Type Germanium Detector, and Its Application to Astronomical Gamma-Ray Spectroscopy." IEEE Trans. Nuc. Sci. NS-31 (1): 307-311; 1984.

Kn89 Knoll, G.F. Radiation Detection and Measurement. New York:John Wiley and Sons. Second Edition; 1989.

Ma84 Malm, H.L.; Watt, N.M. "Background Reduction in Germanium Spectrometers: Material Selection, Geometry, and Shielding." Nucl. Inst. and Meth. in Phys. Res. 223: 420-425; 1984.

Mi86 Michel, C.; Emling, H.; Grosse, E.; Azgui, F.; Grein, H.; Wollersheim, H.J.; Gaardhoje, J.J.; Herskind, B. "Monte Carlo Simulation of Complex Germanium Detector Systems and Compton Suppression Spectrometers." Nuc. Inst. and Meth. in Phys. Res. A251: 119-133; 1986.

Pa68 Palms, J.M.; Wood, R.E.; Strauss, M.G. "A Ge(Li) Duode Spectrometer for Compton Suppression." IEEE Trans. Nuc. Sci. NS-15 (3): 397-398; 1968.

Re84 Reeves, J.H.; Hensley, W.K.; Brodzinski, R.L.; Ryge, P. "An Ultra Low Background Germanium Gamma-Ray Spectrometer Using Super Clean Materials and Cosmic Ray Anticoincidence." IEEE Trans. Nuc. Sci. NS-31 (1): 697-700; 1984.

Re85 Reeves, J.H.; Hensley, W.K.; Brodzinski, R.L. "Second Generation Ultralow Background Germanium Gamma-Ray Spectrometer Using Super Clean Materials and Improved Multilayered Cosmic Ray Anticoincidence and Passive Shielding." IEEE Trans. Nuc. Sci. NS-32 (1): 29-30; 1985.

Va84 Varnell, L.S.; Ling, J.C.; Mahoney, W.A.; Jacobson, A.S.; Pehl, R.H.; Goulding, F.S.; Landis, D.A.; Luke, P.N.; Madden, N.W. "A Position-Sensitive Germanium Detector for Gamma-Ray Astroncmy." IEEE Trans. Nuc. Sci. NS-31 (1): 300-306.; 1984

Ve86 Verplancke, J.; Schoenmaekers, W.; Hesselink, W.H.A.; Hacquebord, A.; Penninga, J.; Stolk, A. "A HPGe-Telescope as Compton Suppression Spectrometer." IEEE Trans. Nuc. Sci. NS-33 (1): 340-342; 1986.

Wa70b Walker, D.M.; Palms, J.M. "Monte-Carlo Analysis of a Ge(Li) Detector Used in the Sum-Coincidence Mode." IEEE Trans. Nuc. Sci. NS-17: 296-297; 1970.

2. MONTE CARLO MODEL PREDICTIONS

2.1. Purpose of Model

Section 1.0 above described the logic supporting the judgment that certain kinds of event sequence discrimination might improve appreciably the performance of gamma ray spectrometers. Because of the complex scattering relationships and pathways in a typical gamma interaction sequence, it is impossible to intuitively predict the results of multiple scattering behavior in a semiconductor detector. Thus, a practical theoretical or experimental approach was needed for the study. Especially at Phase I, it would have been prohibitively expensive and difficult to build detector and electronic systems to identify and test any significant number of promising approaches. In addition, in searching the literature cited in Section 1.1.4, it was noted that several of the experimental systems which have been built were designed based on an intuition of what might be effective, without any systematic exploration of alternatives. Given the current accessibility and low cost of even fairly intensive computing, it now seems more methodical to study the possibilities mathematically before building actual systems.

One effective computational approach for complex nuclear interaction phenomena is Monte Carlo modeling. In this method equations for probability distributions and physical behavior of all scattering processes of interest in the detector are written into the code. Random numbers are then used to select from the probability distributions to determine the path and interaction sequence of individual gammas incident on the "detector". By following a large number of incident gamma rays through their entire interaction sequence, a statistically valid scattering pattern and detector output can be calculated by the Monte Carlo model.

The present research used a Monte Carlo mathematical model of a germanium detector crystal to search for and test event sequence discrimination methods which might be incorporated into hardware at later phases of development. The model (which is described in Appendix B) was an effective means of narrowing the range of possible options and channeling the scope of intuition. The ability to examine the performance of a model detector at the microscopic level permitted the identification of the more effective methods discussed in Section 3.0. Conversely, a number of possible event sequence discrimination methods which seemed reasonable proved to be relatively ineffective (or even counter-productive) when modeled.

2.2. Monte Carlo Results

2.2.1. Calculations Performed

The computer model described in Appendix B was used to simulate energy deposition in a solid, cylindrical HPGe detector crystal for five different monoergetic point sources. All sources were located at 10 cm from the detector. The five particular energies used were chosen to cover the range of interest, and to match the energies of certain isotopic gamma emitters; this would permit the calculated results to be compared to experimental results at a later stage. The energies used were the following:

Energy	Matching Nuclide
88 keV	Cd/Ag-109
320 keV	Cr-51
661 keV	Cs/Ba-137
1115 keV	Zn-65
1836 keV	Y-88

Except for Y-88, all these radionuclides are monenergetic gamma emitters, which would facilitate the comparison between calculational and experimental results.

The crystal size used was 6.0 cm diameter, by 8.0 cm thick. Smaller crystals could be simulated from the event sequence files developed for this size, by terminating each sequence on the occurrence of any event outside the boundaries of the desired smaller crystal. However, this was not deemed necessary for the Phase I calculations: the 6 by 8 cm size being representative of current real detectors, it was used for all studies reported here.

2.2.2. Data Presentations Used

The event sequence files produced by the calculations described above were parsed using custom C-language programs to obtain data presentations which could help the researchers look for regularities and trends. The data were manipulated in several different ways:

1. Event Sequence Listings. The parsing program permits the listing of all event sequences. It was soon found to be more illuminating to examine only certain sequences, specifically the ones which the spectrometer should favor (full-energy sequences), and those which the system should suppress (sequences depositing energy in one of the lower-energy peak regions). Examples of these selected sequence listings are shown in Figures 2-1, 2-2, and 2-3.

Figure 2-1. Selected-Event Sequence Listing:
Sequences Depositing About 88 keV
for Incident Gamma Energy of 661 keV

List of all Events For Energy Deposited In 86 -> 89 keV Range
Energy: 661.00 keV Randomize Seed: 6050
Source to Detector Distance: 10.00 cm
Detector Thickness: 8.00 cm Radius: 3.00 cm

			R	Z
1	Compton	87.01 keV	2.93 cm	0.89 cm
2	Compton	87.41 keV	1.00 cm	6.70 cm
3	Compton	87.52 keV	2.95 cm	0.70 cm
4	Compton	86.97 keV	2.56 cm	1.56 cm
5	Compton	87.44 keV	0.66 cm	3.45 cm
6	Compton	86.89 keV	2.68 cm	3.12 cm
7	Compton	86.54 keV	1.92 cm	1.84 cm
8	Compton	88.58 keV	2.01 cm	0.23 cm
9	Compton	88.86 keV	2.34 cm	4.20 cm
10	Compton	87.76 keV	2.90 cm	0.23 cm
11	Compton	86.42 keV	1.77 cm	1.57 cm
12	Compton	10.53 keV	1.63 cm	2.53 cm
	Compton	14.96 keV	2.40 cm	5.30 cm
	Compton	61.72 keV	2.45 cm	5.40 cm
13	Compton	86.42 keV	2.60 cm	4.25 cm
14	Compton	23.84 keV	1.05 cm	0.22 cm
	Compton	64.07 keV	1.49 cm	1.78 cm
15	Compton	88.07 keV	2.64 cm	0.85 cm
16	Compton	87.13 keV	2.09 cm	7.32 cm
17	Compton	86.18 keV	2.18 cm	1.11 cm
18	Compton	87.05 keV	1.86 cm	1.27 cm
19	Compton	30.23 keV	2.72 cm	0.71 cm
	Compton	55.84 keV	2.72 cm	0.73 cm
20	Compton	86.38 keV	2.94 cm	0.11 cm

Figure 2-2. Selected-Event Sequence Listing: Sequences Depositing About 661 keV for Incident Gamma Energy of 1836 keV

List of all Events For Energy Deposited In 651 -> 666 keV Range
Energy: 1836.00 keV Randomize Seed: 4567
Source to Detector Distance: 10.00 cm
Detector Thickness: 8.00 cm Radius: 3.00 cm

			R	Z
1	Compton	651.49 keV	1.64 cm	4.48 cm
2	Compton	655.17 keV	2.65 cm	1.43 cm
3	Compton	662.95 keV	2.86 cm	4.95 cm
4	Compton	660.97 keV	1.14 cm	7.54 cm
5	Compton	652.83 keV	2.20 cm	1.75 cm
6	Compton	664.42 keV	2.49 cm	1.55 cm
7	Compton	656.83 keV	1.89 cm	2.41 cm
8	Compton	662.29 keV	2.15 cm	2.72 cm
9	Compton	138.14 keV	2.27 cm	0.21 cm
	Compton	526.94 keV	2.34 cm	7.46 cm
10	Compton	652.16 keV	2.61 cm	0.00 cm
11	Compton	652.83 keV	2.83 cm	4.27 cm
12	Compton	584.75 keV	0.81 cm	2.12 cm
	Compton	72.74 keV	1.07 cm	2.87 cm
13	Compton	504.35 keV	2.12 cm	0.83 cm
	Compton	158.93 keV	1.70 cm	2.56 cm
14	Compton	654.84 keV	0.72 cm	1.46 cm
15	Compton	661.13 keV	1.93 cm	2.62 cm
16	Compton	552.92 keV	2.24 cm	3.06 cm
	Compton	107.06 keV	2.30 cm	4.46 cm
17	Compton	664.09 keV	2.74 cm	0.27 cm
18	Compton	659.32 keV	2.24 cm	4.95 cm
19	Compton	586.43 keV	1.33 cm	4.05 cm
	Compton	77.66 keV	1.48 cm	5.90 cm

Figure 2-3. Selected-Event Sequence Listing: Sequences Depositing About 661 keV for Incident Gamma Energy of 661 keV

List of all Events For Energy Deposited in 651 -> 666 keV Range
Energy: 661.00 keV Randomize Seed: 6050
Source to Detector Distance: 10.00 cm
Detector Thickness: 8.00 cm Radius: 3.00 cm

			R	Z
1	Compton	167.39 keV	1.17 cm	2.77 cm
	Compton	246.34 keV	1.39 cm	2.97 cm
	Compton	6.06 keV	1.31 cm	3.14 cm
	Compton	85.69 keV	1.46 cm	3.22 cm
	Photo-Electric	154.92 keV	1.52 cm	2.95 cm
2	Compton	427.72 keV	1.52 cm	2.28 cm
	Photo-Electric	233.28 keV	1.10 cm	2.14 cm
3	Compton	242.20 keV	1.15 cm	0.40 cm
	Compton	64.73 keV	0.31 cm	1.33 cm
	Compton	109.43 keV	0.20 cm	1.90 cm
	Photo-Electric	244.63 keV	0.52 cm	2.09 cm
4	Compton	351.82 keV	1.31 cm	2.11 cm
	Compton	140.95 keV	0.82 cm	2.26 cm
	Photo-Electric	168.23 keV	0.63 cm	1.75 cm
5	Compton	395.16 keV	1.82 cm	1.45 cm
	Photo-Electric	265.84 keV	2.52 cm	1.22 cm
6	Compton	393.76 keV	0.86 cm	2.69 cm
	Compton	90.86 keV	1.47 cm	2.56 cm
	Compton	42.20 keV	1.49 cm	2.19 cm
	Compton	19.41 keV	2.31 cm	3.05 cm
	Photo-Electric	114.77 keV	2.73 cm	3.06 cm
7	Compton	326.21 keV	2.84 cm	2.41 cm
	Compton	169.66 keV	2.36 cm	3.04 cm
	Compton	19.55 keV	2.39 cm	1.03 cm
	Photo-Electric	145.58 keV	2.39 cm	0.06 cm
8	Compton	450.87 keV	2.55 cm	3.49 cm
	Compton	75.44 keV	2.32 cm	2.99 cm
	Photo-Electric	134.69 keV	2.37 cm	3.06 cm
9	Photo-Electric	661.00 keV	2.70 cm	2.20 cm
10	Compton	464.31 keV	2.32 cm	3.84 cm
	Compton	12.39 keV	1.04 cm	1.53 cm
	Photo-Electric	184.30 keV	1.30 cm	1.35 cm

The sequences in Figure 2-1 show that almost all event sequences that deposit background counts at about 88 keV (for 661 keV initial energy gammas) consist of a single Compton event (followed by escape). This is reasonable, since it would be less probable to have more than one scatter that would deposit so little energy each as to add up to 88 keV. But Figure 2-2 shows the prominence of single-scatter sequences in producing continuum counts, even in the 661 keV peak region.

By contrast, Figure 2-3 shows the extreme rarity of first-event photoelectric interactions for 661 keV incident gammas, even when one considers only those sequences leading to full-energy absorption. The data in Figure 2-3 are a statistically poor sample of the results for full-energy sequences at 661 keV, but when the complete data set is examined, it is found that less than 6% of the 661-keV full-energy sequences consist of a first-event photoelectric interaction.

2. Event Number Distributions. The subjective impressions regarding numbers of scattering events were confirmed by histogram data produced by the parsing program. For example, the number of events in escape sequences is shown (as a function of initial gamma energy) in Figure 2-4. These data confirm that sequences in which only part of the gamma energy is absorbed are almost all composed of one or two Compton scatters at all energies. As might be expected, the share of one-scatter escape sequences is highest at low energy.

The corresponding distributions for sequences in which the full gamma energy is absorbed are shown in Figure 2-5. At 88 keV, where photoelectric interactions predominate, almost all full-energy absorption sequences consist of one photoelectric event. However, at all higher energies calculated, sequences of 2 to 4 events (including the final absorption) are most common. Note that the total number of events occasionally exceeds 10, although the proportion of sequences with 8 or more events is less than 3% at all energies shown.

From these two graphs, it may be concluded that (except for very low energies) almost all one-event sequences lead to continuum counts rather full-energy peak counts. The same is true of most two-event sequences. This clearly suggests that discrimination based on numbers of events might be useful in reducing the Compton continuum.

Figure 2-4. Number of Events in Sequences Ending in Escape of a Scattered Gamma

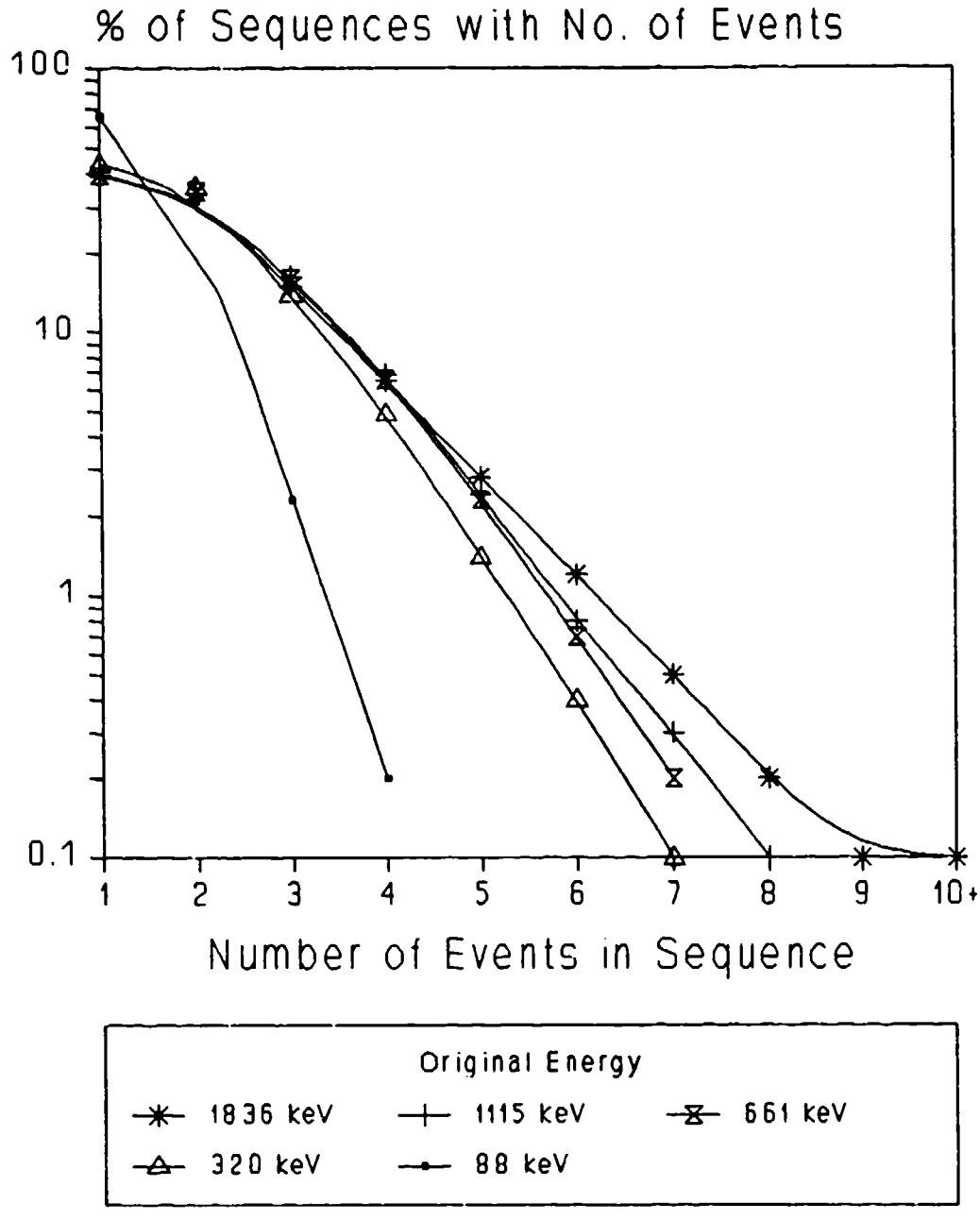

Figure 2-5. Number of Events in Sequences Ending in Full-Energy Absorption

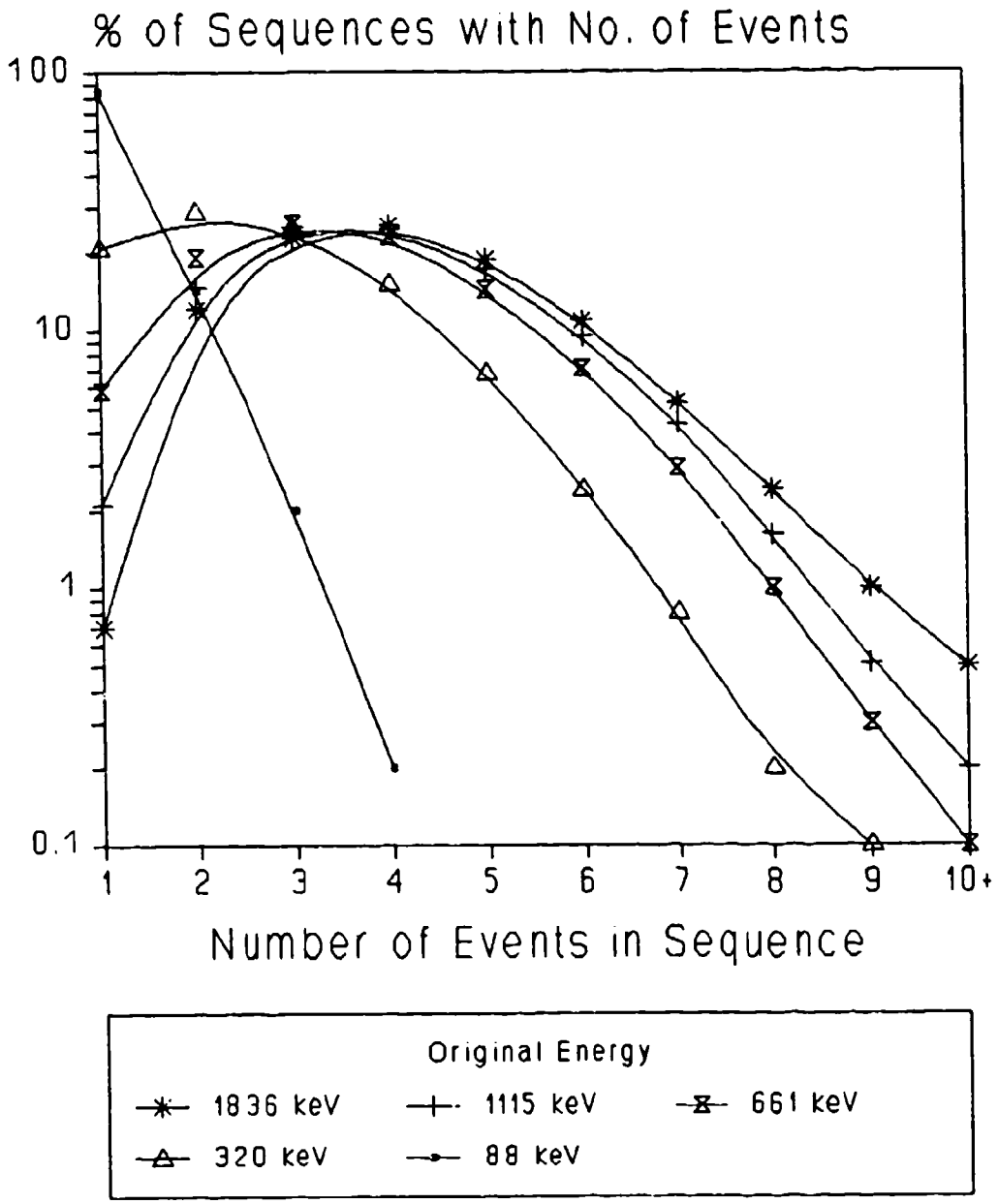

3. Event Spatial Distribution Histograms. The parsing programs could also produce tabulations showing the spatial distribution of selected events within the detector volume, according to radial distance from the detector axis and depth into the detector. (An example of one of these tabulations is shown in Figure 2-6.)

   Spatial tabulations were prepared and studied for the following types of events:

   a. All events in sequences that end in full-energy absorption

   b. All events in sequences that end in escape

   c. First-event Compton scatters

   d. Second-event Compton scatters (preceded by initial Compton)

   e. Third-event Compton scatters (preceded by all Comptons)

   f. Fourth-event Compton scatters (preceded by all Comptons)

   g. Fifth-event Compton scatters (preceded by all Comptons)

   These data may also be presented graphically. For example, Figures 2-7 and 2-8 show the distributions of all events in escape sequences and in full-energy sequences, respectively, for the same energy (320 keV). The two distributions are not mirror images of each other, but they are distinctly different. They show (not only at 320 keV, but at all energies studied) that events in full-energy sequences are weighted toward the center of the detector, while escape sequences have more events in the top and side surfaces of the detector. This clearly suggests that discrimination based on spatial distribution of events might be useful in reducing the Compton continuum.

4. Spectrum Lists and Plots. Whatever parsing algorithm was used, the parsing program created a tabulation of the number of sequences producing a given energy deposition in the crystal. This type of histogram is equivalent to a gamma ray spectrum from a spectrometer operating in accordance with the rules embodied in the parser. Data were available in both tabular listing and conventional plotted form.

Figure 2-6. Example Tabulation of the Spatial Distribution of Selected Events

Distribution of all events that end in ESC
Energy: 320.00 keV Randomize Seed: 5345
Source to Detector Distance: 10.00 cm
Detector Thickness: 8.00 cm Radius: 3.00 cm

Distances are in mm

Zv R>	0-> 2	2-> 4	4-> 6	6-> 8	8-> 10	10-> 12	12-> 14	14-> 16
0-> 5	41	176	259	367	465	587	716	827
5-> 10	18	61	131	169	251	253	310	413
10-> 15	12	38	62	102	125	148	229	248
15-> 20	7	21	51	66	104	122	144	185
20-> 25	5	23	37	54	61	78	97	133
25-> 30	5	10	16	28	45	69	86	72
30-> 35	2	8	25	33	41	46	65	84
35-> 40	3	14	9	19	24	48	51	57
40-> 45	1	9	11	10	17	26	37	43
45-> 50	3	3	5	10	13	27	21	33
50-> 55	2	5	2	12	10	10	15	33
55-> 60	2	2	9	8	11	14	10	14
60-> 65	1	3	4	4	6	8	11	24
65-> 70	2	7	8	10	5	3	12	16
70-> 75	0	3	7	6	5	9	11	14
75-> 80	2	1	5	9	12	13	17	12

Distances are in mm

Zv R>	16-> 18	18-> 20	20-> 22	22-> 24	24-> 26	26-> 28	28-> 30	% of Total
0-> 5	955	1113	1329	1495	1740	1968	2268	32.661
5-> 10	531	621	726	898	1080	1274	1587	51.663
10-> 15	348	385	470	590	749	961	1186	64.569
15-> 20	229	253	344	385	521	694	813	73.562
20-> 25	159	197	255	294	422	486	661	80.325
25-> 30	104	157	190	207	273	338	500	85.119
30-> 35	72	108	146	166	188	270	330	88.735
35-> 40	83	84	115	139	168	214	261	91.678
40-> 45	55	61	84	108	142	174	194	93.897
45-> 50	43	49	66	74	107	97	162	95.525
50-> 55	32	45	52	55	67	88	104	96.740
55-> 60	22	34	22	34	54	85	78	97.651
60-> 65	19	18	32	50	43	42	65	98.404
65-> 70	14	17	30	28	38	42	34	99.011
70-> 75	17	20	25	24	28	26	33	99.532
75-> 80	13	17	17	15	20	24	28	100.000

Total # of Events: 43801

Figure 2-7. Spatial Distribution of
All Events in Sequences Ending in
Escape of a Scattered Gamma
(Initial Energy = 320 keV)

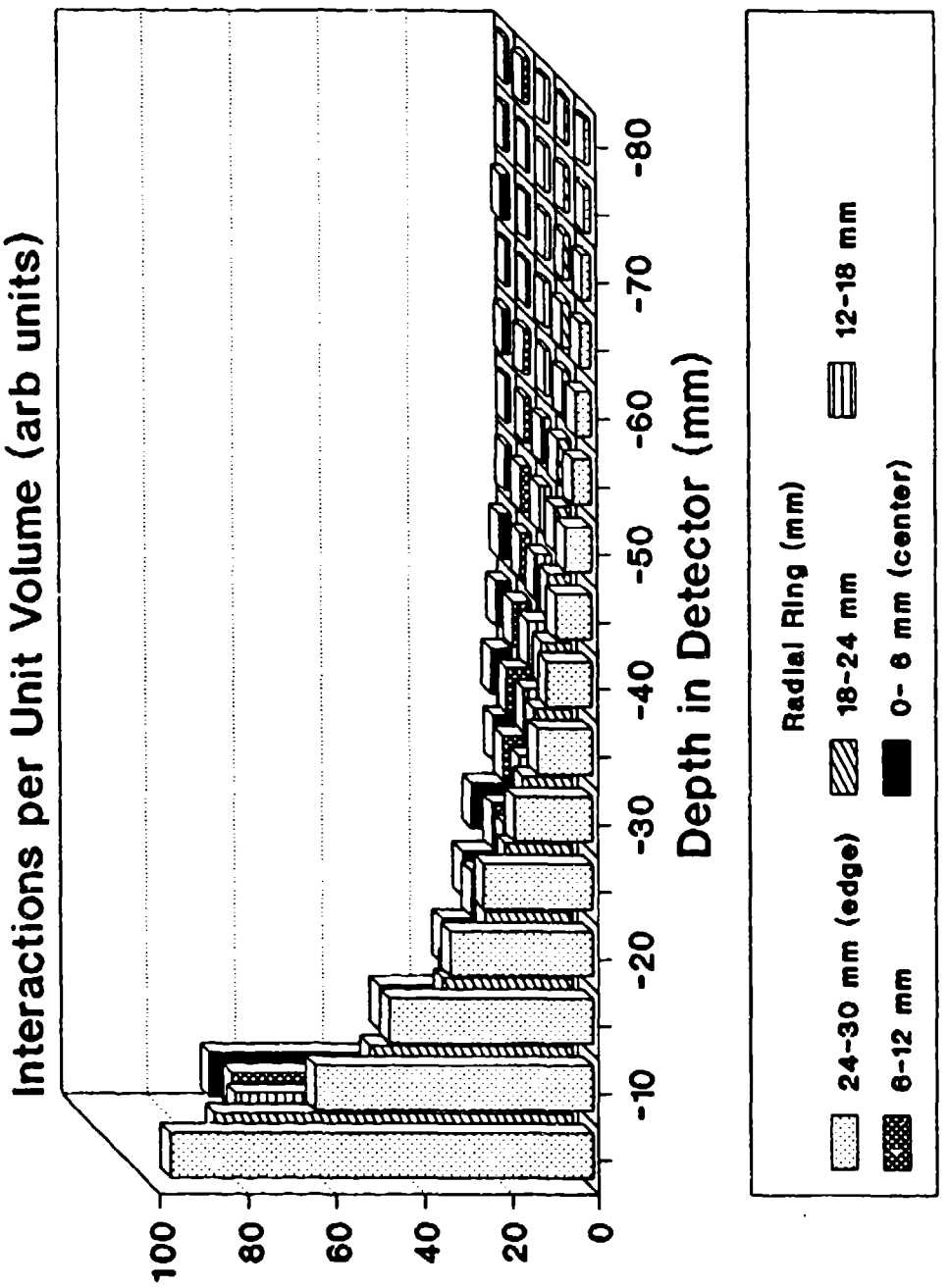

Figure 2-8. Spatial Distribution of
All Events in Sequences Ending in
Full-Energy Absorption
(Initial Energy = 320 keV)

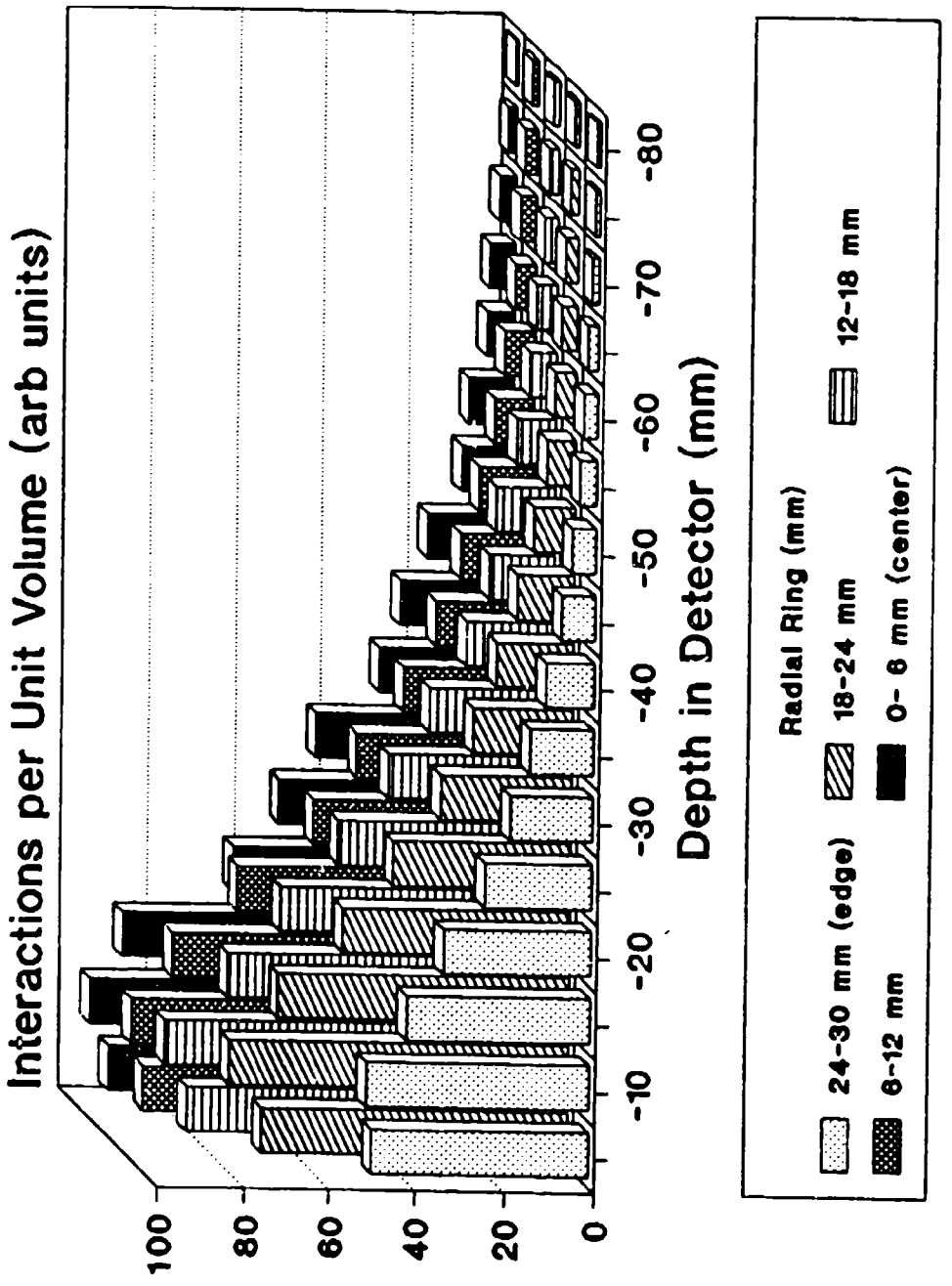

Figure 2-9 is an example spectrum plot: the spectrum for a normal spectrometer (i.e., one with no event discrimination), responding to 1115-keV gammas. (Note the logarithmic count scale.) It correctly reproduces the full-energy peak at 1115 keV, the pair production escape peaks at 93 keV and 604 keV, the Compton edge at about 900 keV, the continuum below the edge, and the valley above the edge. The roughness of the continuum is appropriate to the Poisson variability of the moderate number of counts per channel (30 - 100).

Some comments are in order regarding the differences in appearance between this calculated spectrum and the spectrum which one would expect to observe in a real measurement:

a. The peaks (full-energy and escape) are perfectly resolved in the calculated spectrum. This is because the model does not include the effects which lead to peak broadening in real spectrometers. These effects include statistical variations in the numbers of charge carriers produced per unit energy deposited; statistical variations in the fraction of the produced charge carriers that are finally collected; and the baseline electronic noise in the system.

b. The continuum does not rise toward the low-energy end in the calculated spectrum. This is because the model does not include the effects of electrical noise and cosmic ray background, which are primarily responsible for the continuum rise observed in real spectrometers.

c. The Compton valley is completely empty in the calculated spectrum. Two kinds of sequences contribute to counts in the valley of spectra on a real spectrometer. The first contribution is continuum counts from cosmic background events and from higher-energy gamma rays in the sample. Neither of these effects is included in the model.

Figure 2-9. Calculated Spectrum for Detector Operating in Normal Mode (Initial Energy = 1115 keV)

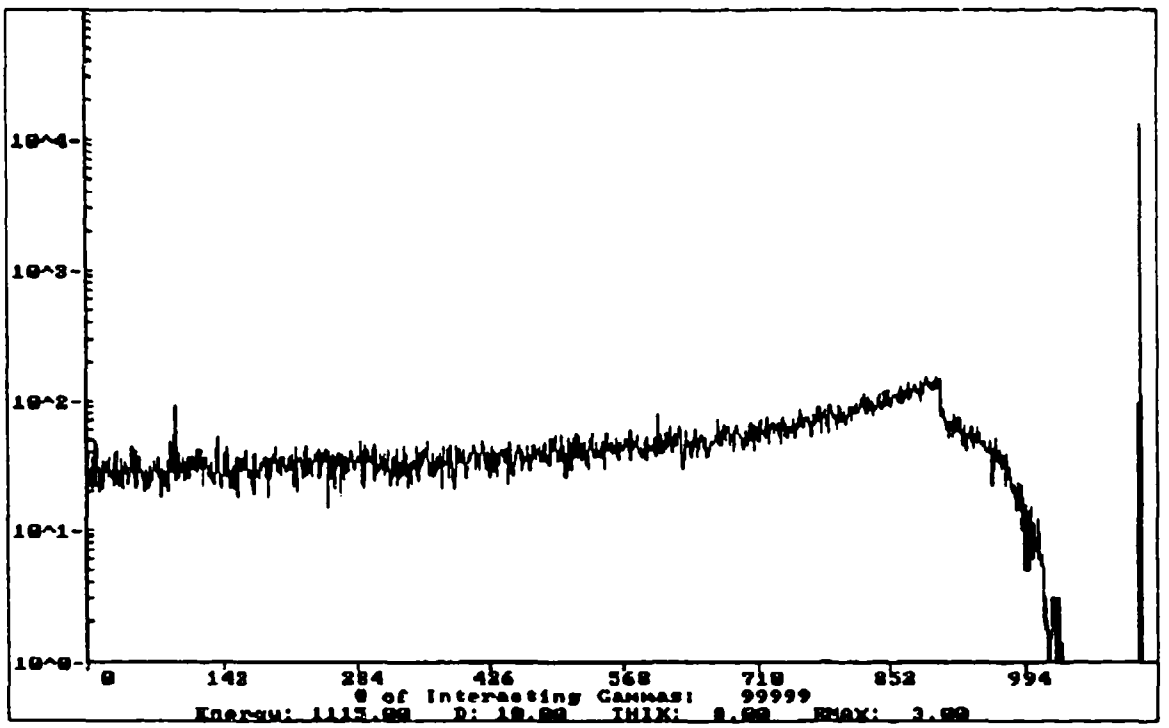

The second contribution is the very rare sequence in which the incident gamma scatters many times in the detector and a scattered gamma escapes, bearing a very small fraction of the original energy. This effect is correctly accounted for in the model. To get a count very near the full-energy peak, the sequence would have to end in the escape of a gamma ray with energy of only a few keV; but as discussed in Appendix A, such photons have sub-millimeter pathlengths in germanium. Therefore, although such an event might happen, it would be extremely rare. The valley should be almost empty on the peak side, and have a very sharp slope on the edge side, as shown in the example spectrum. With a large enough number of interacting gammas, a count might be recorded even on the peak side, but this did not occur in any of the runs performed in this research.

The correspondence of the calculated spectrum to observed spectra, except for a small number of explicable effects, lends credibility to the correctness of the model and parser programs for this study of event sequence analysis.

5. Pathlength Histograms. The model results were parsed to develop data on the in-detector pathlength of gamma rays between events (including the pathlength before the initial event). A summary of these data for 320-keV incident gammas is given in Figure 2-10; the results are typical of those at all five energies, and for all pathlength classes.

Comparison of the data for full-energy sequences to those for partial-absorption sequences shows that the partial-absorption sequences have a somewhat larger proportion of short pathlengths. The difference prevails in both in the 0-15 mm and 15-30 mm classes, although it is more pronounced in the 0-15 mm class. This finding further encourages the expectation that escape sequences will have more localized energy deposition than will full-energy sequences.

Figure 2-10. Pathlength Comparison for Escape and Full-Energy Sequences (Initial Energy = 320 keV)

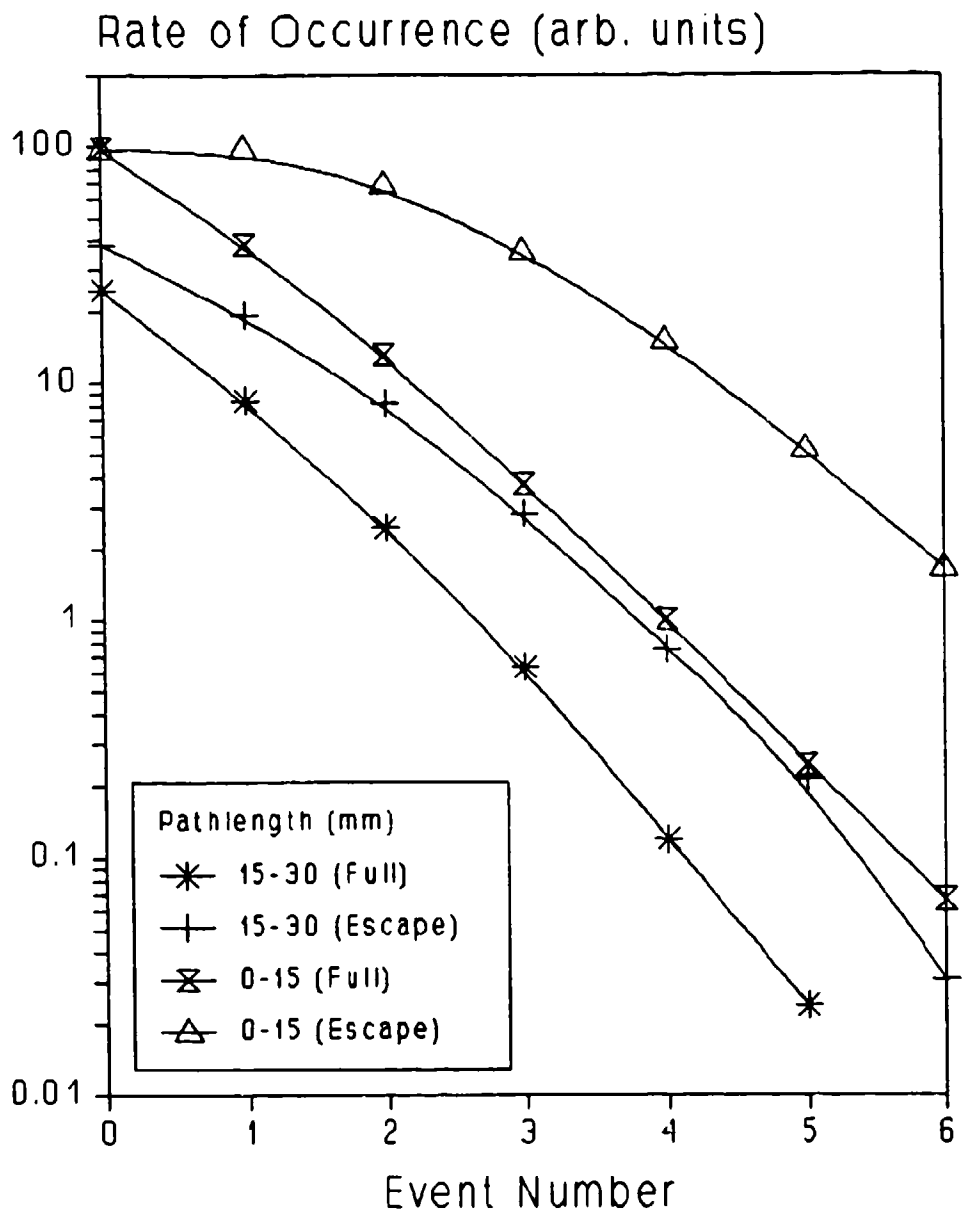

2.2.3. Event Sequence Discriminators Selected for Further Study

The discussion of data presentations in Section 2.2.2 demonstrated that the Monte Carlo model predicts significant differences between event sequences resulting in full and partial absorption of the incident gamma energy. The major differences noted are the following:

1. Above the very low energy range where photoelectric events dominate, the more interaction events in an event sequence, the more likely the sequence is to produce a full-energy count rather than a continuum count. This situation may be expressed using a break-even event number. At a given energy, if an event sequence has at least the break-even number of events, it is more likely to be a full-energy sequence than a partial-energy sequence. For the five energies studied, the break-even number of events is as follows:

Original Energy (keV)	Break-Even Number of Events
88	1
320	1 to 2
661	2 to 3
1115	3 to 4
1836	3 to 4

2. A partial-energy sequence is more likely than a full-energy sequence to have interaction events in the top and sides of the crystal. Full-energy sequences have their events more confined to the center of the detector.

3. Partial-energy sequences have an above-average proportion of short pathlengths through the detector between interaction events. Combined with the fact that they have fewer interaction events, this leads to the expectation that the more dispersed energy is within the detector crystal, the more likely the responsible interaction sequence is to be a full-energy sequence.

From the above facts it is possible to propose several different types of event sequence discriminators that seem likely to improve gamma ray spectrometer performance. In Phase I of the present research, the following types of discriminators were tested on the results of the Monte Carlo model:

1. Those that accept only sequences in which all the events occur in the top of the crystal.

2. Those that accept only sequences in which all the events occur toward the core of the crystal.

3. Those that accept only sequences in which there are at least some set minimum number of events.

Results of tests of criteria of the above three types are reported in Section 3.0.

3. EFFECT OF SELECTED EVENT SEQUENCE DISCRIMINATORS ON PREDICTED SPECTRA

3.1. Event Location Discriminators

Two major types of event location discriminators were tested: those which accept only sequences confined to the top of the detector, and those which accept only sequences confined to the core of the detector. The particular discriminators tested during Phase I, and their effects on the predicted gamma spectra, are discussed below.

3.1.1. Accept Sequences Confined to Top 10 mm of Detector

A simple discriminator which should suppress the Compton continuum is this: accept only those event sequences in which all the events occur in the top 10 mm of the detector. This amounts to using the remainder of the detector as a Compton suppression spectrometer, since any sequences which include one or more events in the lower part of the detector will be rejected for counting. This discriminator was tested during Phase I (and is called discriminator z6 in the project records).

As expected, this discriminator markedly reduces the continuum level, regardless of the incident gamma ray energy. For example, Figure 3-1 compares the Compton continuum produced by 661-keV incident gammas under two conditions: (a) accept all sequences for counting, as a normal spectrometer does; and (b) accept only those sequences with no events below 10 mm into the detector. In this particular case, the continuum counts per channel are reduced by a factor between 2.5 and 3 by the new criterion. The data for all cases in Table 3-1 show that (depending on the incident energy and the peak region of interest energy) the "Accept Top 10 mm" discriminator reduces the continuum level to 20% to 40% of its level in a normal spectrum.

However, the continuum reduction is also accompanied by a reduction in the peak efficiency at all energies, since some events leading to a final photoelectric absorption occur throughout the detector. Because higher energies produce events more dispersed in the detector, the efficiency reduction is greater as incident gamma energy increases. The data in Table 3-1 confirm this effect: at 88 keV, the efficiency reduction is only 2%, but at 1836 keV, the reduction is 90%.

Figure 3-1. Compton Continuum for
661-keV Incident Gammas,
Under the "Accept Top 10 mm" Discriminator

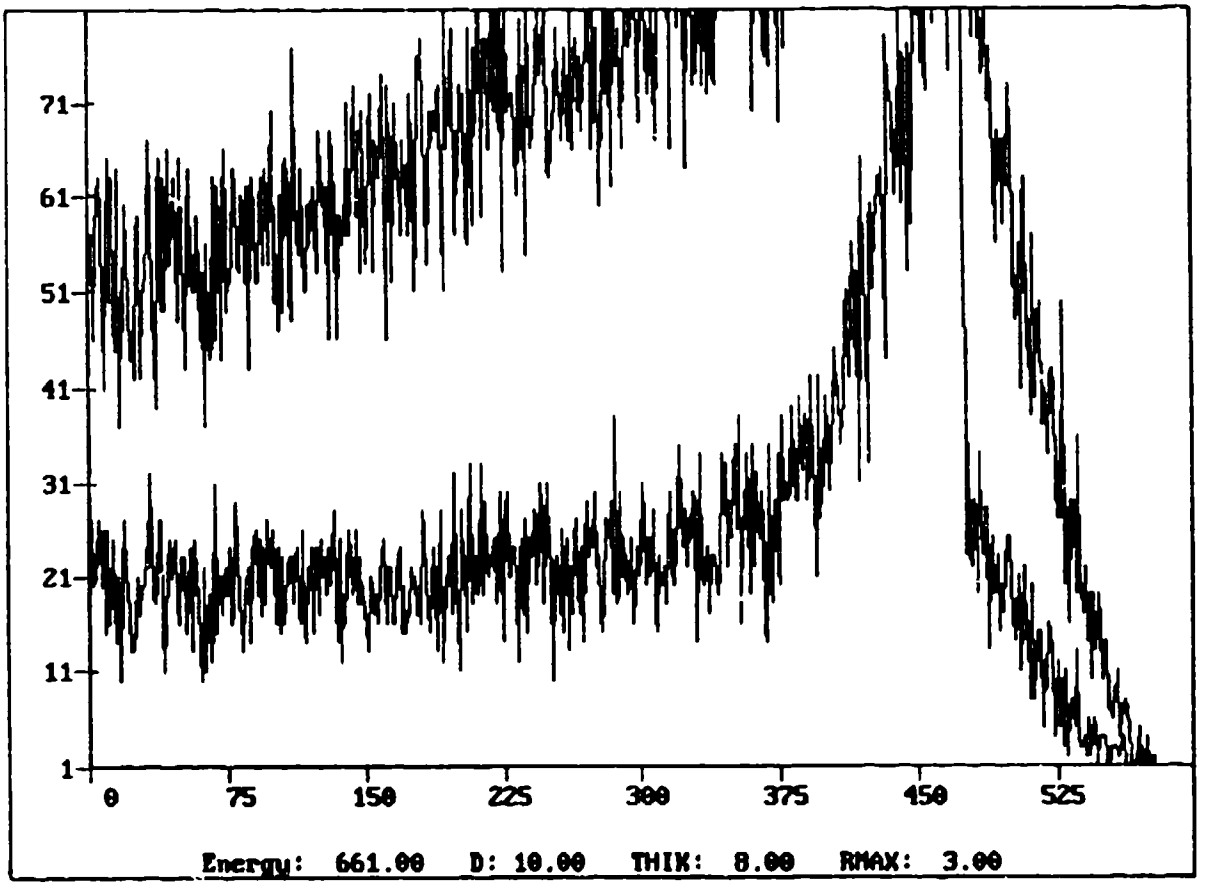

Top curve: Accept all sequences ("Normal" spectrum).
Bottom curve: Reject sequences with any events below 10 mm into the detector.

Table 3-1. Results of the "Accept Top 10 mm" Discriminator

Continuum Level Under Discriminator:
(Normal Continuum in Region of Interest = 100)

Incident Gamma Energy (keV)	Region of Interest Energy (keV)			
	88	320	661	1115
88	(N/A)	(N/A)	(N/A)	(N/A)
320	42	(N/A)	(N/A)	(N/A)
661	37	30	(N/A)	(N/A)
1115	31	28	23	(N/A)
1836	32	28	22	24

Peak Counting Efficiency Under Discriminator:
(Normal Efficiency at Given Energy = 100)

Incident Gamma Energy (keV)	Normalized Efficiency
88	98
320	31
661	17
1115	12
1836	10

Counting Time Required Under Discriminator:
(Normal Counting Time for Conditions = 100;
counting times less than 100 represent improved sensitivity)

Desired Peak Energy (keV)	Interfering Gamma Energy (keV)			
	320	661	1115	1836
88	66	62	56	57
320	(N/A)	176	171	170
661	(N/A)	(N/A)	132	131
1115	(N/A)	(N/A)	(N/A)	131
1836	(N/A)	(N/A)	(N/A)	(N/A)

The net result of the tradeoff between the two effects (reduction in continuum and reduction in efficiency) may be quantified using the sensitivity. Equations developed in section 2.7 showed that at a given energy for which the background is B and the efficiency is ϵ, the spectrometer sensitivity is proportional to $(\sqrt{B})/\epsilon$. That is, given a desired level of net activity to be detected, and an acceptable level of uncertainty in the assay, the counting time required to perform the assay <u>increases</u> as $\sqrt{B}$, and <u>decreases</u> as $1/\epsilon$. An event discrimination criterion is successful only to the extent that it reduces this required counting time for a given level of net signal.

Note that the efficiency and background are for different incident gamma ray energies. Calculated relative sensitivity for analysis of a radionuclide with full energy gamma rays of energy E_1 in the presence of interference counts generated by higher energy gamma rays of energy E_2 would be based on efficiency (ϵ) at E_1 and background counts (B) at E_1 produced by the higher energy gamma ray of incident energy E_2.

Thus, if a specific higher energy gamma ray is not of quantitative interest, then reduction of the full energy peak efficiency for that gamma ray is of no concern, but only reduction in the lower energy background contribution from the gamma ray. By calculation the relative sensitivity at E_1 for various values of E_2, a matrix is generated which allows evaluation for a range of interference energies as experienced in many applications.

Table 3-1 presents the predicted net counting time change required to achieve a specified sensitivity by the "Accept Top 10 mm" discriminator. (Note that since Monte Carlo calculations were not performed for any energies higher than 1836 keV, continuum levels B at 1836 keV are not available. Therefore, counting time changes cannot be calculated for 1836 keV.) The tabulated data show that the tradeoff produced by the "Accept Top 10 mm" discriminator is an improvement only for the lowest peak energies: at 88 keV, the predicted counting time required for a given sensitivity <u>decreases</u> by about 40%, whereas for other peak energies the required counting time <u>increases</u> by 30% to 75%.

The conclusion is then that the "Accept Top 10 mm" criterion would give improved sensitivity at low energies (less than about 100 keV), but would reduce the sensitivity for higher energy peaks. The active region of a detector operated under this discriminator might well be smaller than that of the planar detectors commonly used to detect low-energy peaks in the presence of higher-energy gamma emitters; even so, its sensitivity should be better than that of the planar detector, because of its marked Compton suppression.

3.1.2. Accept Sequences Confined to Top 5 mm of Detector

If it is low-energy gammas which are to be detected in the presence of interference produced by higher-energy gammas, is the "Accept Top 10 mm" discriminator the best that can be used, or might other thicknesses produce even better results? To answer this question, a second discriminator was tested: accept only those event sequences in which all the events occur in the top 5 mm of the detector. (This "Accept Top 5 mm" discriminator is called discriminator z9 in the project records).

As Figure 3-2 shows, the continuum reduction under the "Accept Top 5 mm" discriminator is even greater than under the "Accept Top 10 mm" discriminator. This is to be expected, since some additional sequences must be rejected under the more restrictive discriminator. It would also be expected that there will be a greater efficiency reduction. This also proves to be the case, particularly at higher energies, as shown in the tradeoff data in Table 3-2.

For the lowest energy, the "Accept Top 5 mm" discriminator is an improvement over the "Accept Top 10 mm" discriminator. Comparison of Tables 3.1-1 and 3.1-2 shows that the predicted count time required for a given sensitivity at 88 keV decreases from about 65% of the normal time under the "Accept Top 10 mm" discriminator, to about 55% of the normal time under the "Accept Top 5 mm" discriminator. At all other energies, however, the "Accept Top 5 mm" discriminator increases the required counting times immensely: the predicted increase in counting time at 1115 keV is more than a factor of 11.

The results in the two tables support the following conclusions: (a) the "Accept Top 5 mm" discriminator is superior to the "Accept Top 10 mm" discriminator for low energy gammas; and (b) the range of beneficial application of this technique would be the detection of gammas of 100 keV or less in the presence of interference gammas of higher energy.

Figure 3-2. Compton Continuum for
661-keV Incident Gammas,
Under the "Accept Top 5 mm" Discriminator

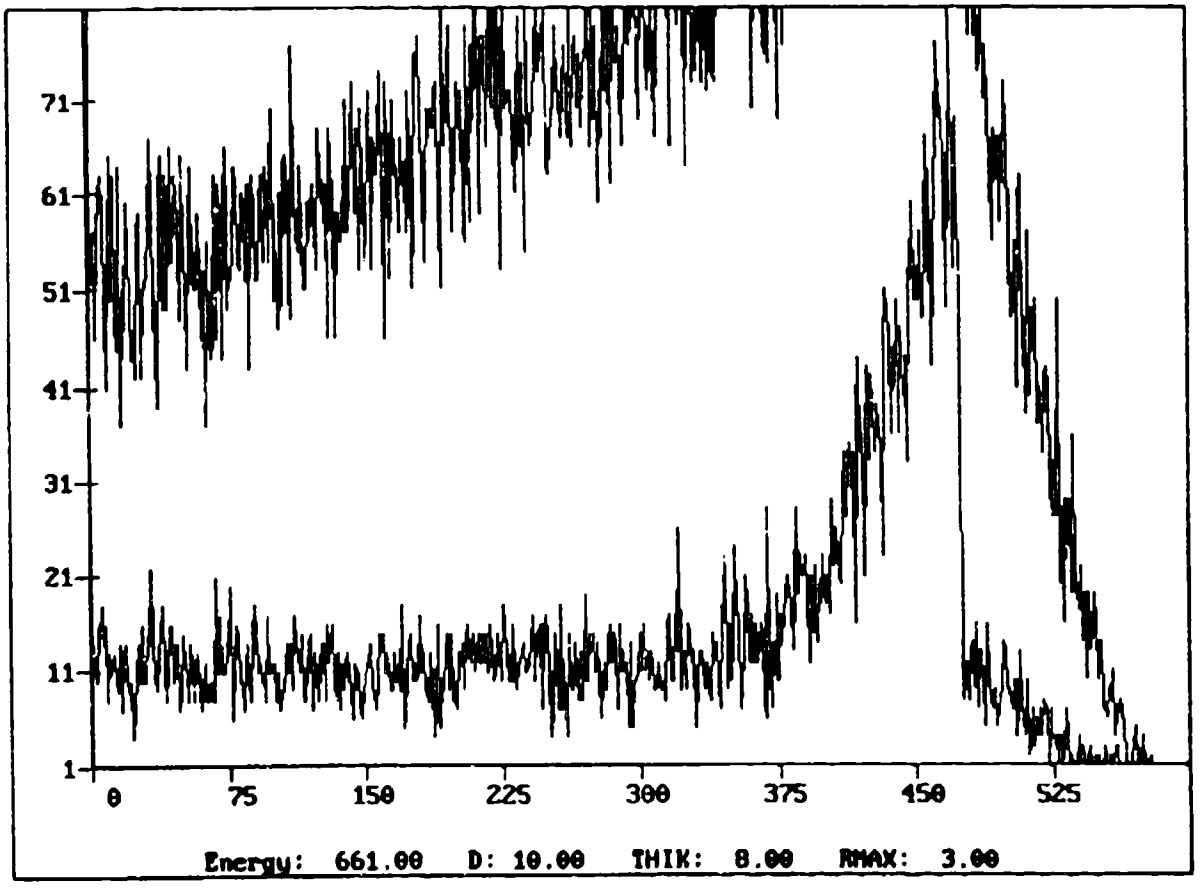

Top curve: Accept all sequences ("Normal" spectrum).
Bottom curve: Reject sequences with any events below 5 mm into the detector.

Table 3-2. Results of the "Accept Top 5 mm" Discriminator

Continuum Level Under Discriminator:
(Normal Continuum in Region of Interest = 100)

Incident Gamma Energy (keV)	Region of Interest Energy (keV)			
	88	320	661	1115
88	(N/A)	(N/A)	(N/A)	(N/A)
320	21	(N/A)	(N/A)	(N/A)
661	23	18	(N/A)	(N/A)
1115	18	17	13	(N/A)
1836	22	12	9	15

Peak Counting Efficiency Under Discriminator:
(Normal Efficiency at Given Energy = 100)

Incident Gamma Energy (keV)	Normalized Efficiency
88	86
320	14
661	6
1115	3
1836	3

Counting Time Required Under Discriminator:
(Normal Counting Time for Conditions = 100;
counting times less than 100 represent improved sensitivity)

Desired Peak Energy (keV)	Interfering Gamma Energy (keV)			
	320	661	1115	1836
88	53	56	49	54
320	(N/A)	301	291	248
661	(N/A)	(N/A)	623	531
1115	(N/A)	(N/A)	(N/A)	1119
1836	(N/A)	(N/A)	(N/A)	(N/A)

3.1.3. Reject Sequences with Events in Outer 6 mm of Detector

Both the "Accept Top 10 mm" and "Accept Top 5 mm" discriminators are based on selecting events based on their depth into the detector as measured along the detector axis. A different type of discriminator would be based on the event position as measured from the detector axis outward. The only discriminator of this type tested during Phase I was the following: reject a sequence if it has any event in the outer 6 mm of the detector. (Note: the 6 mm thickness applied only along the curved side of the cylindrical detector, not along its flat circular faces.) This discriminator (called z5 in the project records) is referred to below as "Reject Outer 6 mm".

Table 3-3 summarizes the results of this discriminator, showing that its effects on both continuum and efficiency are less dramatic than the effects of either the "Accept Top 5 mm" or "Accept Top 10 mm" discriminator. Indeed, although the counting time penalty at higher energies (20% to 30%) is less severe than for the other discriminators, the "Reject Outer 6 mm" discriminator does not produce a significant net performance improvement at any energy tested.

Since the "Reject Outer 6 mm" discriminator produced no encouraging results, no other discriminators based on event radial position were tested during Phase I.

Table 3-3. Results of the "Reject Outer 6 mm" Discriminator

Continuum Level Under Discriminator:
(Normal Continuum in Region of Interest = 100)

Incident Gamma Energy (keV)	Region of Interest Energy (keV)			
	88	320	661	1115
88	(N/A)	(N/A)	(N/A)	(N/A)
320	42	(N/A)	(N/A)	(N/A)
661	42	47	(N/A)	(N/A)
1115	49	51	56	(N/A)
1836	42	53	55	51

Peak Counting Efficiency Under Discriminator:
(Normal Efficiency at Given Energy = 100)

Incident Gamma Energy (keV)	Normalized Efficiency
88	65
320	61
661	57
1115	55
1836	54

Counting Time Required Under Discriminator:
(Normal Counting Time for Conditions = 100;
counting times less than 100 represent improved sensitivity)

Desired Peak Energy (keV)	Interfering Gamma Energy (keV)			
	320	661	1115	1836
88	100	100	108	99
320	(N/A)	114	118	121
661	(N/A)	(N/A)	132	131
1115	(N/A)	(N/A)	(N/A)	131
1836	(N/A)	(N/A)	(N/A)	(N/A)

3.2. Event Number Discriminator

As discussed in Section 2.3, the number of events in an interaction sequence is generally higher for sequences depositing the full gamma energy than for those ending in escape. Specifically, this is true for all except the lowest energies, where a first-event photoelectric absorption has appreciable probability. At all energies where Compton interaction is more probable than photoelectric (that is, above 100-200 keV in germanium), one-event sequences are more likely to deposit only part of the incident energy than they are to deposit the full energy. That is, the break-even number of events (the number of events required to make a sequence as probable to be full-energy as to be partial-energy) is at least two, when the gamma energy is at least a few hundred keV.

In fact, depending on the incident energy, the break-even number of events may be more than two. However, in Phase I only one event number discriminator was tested: reject all sequences having only one event. This discriminator (called z11 in the project records) is referred to below as "Reject One-Event".

Table 3-4 summarizes the results for this discriminator. Continuum suppression is seen to be greatest when the incident gamma energy is high and the region of interest energy is low. Indeed, for a region of interest energy of 88 keV, and incident gamma energies of 1115 keV and 1836 keV, the continuum counts are almost eliminated by the "Reject One-Event" discriminator (see Figure 3-3). For a lower incident energy (e.g., 661 keV), the continuum reduction is appreciable, although not as dramatic (see Figure 3-4).

Because single-event photoelectric sequences are so improbable above about 300 keV, the "Reject One-Event" discriminator has minimal effect on predicted efficiency in that energy range. In fact, as the table shows, the efficiency effect above about 600 keV is negligible. Therefore, except for the lowest peak energy (88 keV), the "Reject One-Event" discriminator is predicted to produce considerable reductions in required counting time: depending on the interfering energy and the peak energy, the predicted improvement exceeds 50%.

The "Reject One-Event" discriminator was found to produce predicted performance improvements for all peak energies above 88 keV. This is in contrast to the event location discriminators discussed above, all of which imply worsened sensitivity at higher energy when compared to normal spectroscopy methods.

Table 3-4. Results of the "Reject One-Event" Discriminator

Continuum Level Under Discriminator:
(Normal Continuum in Region of Interest = 100)

Incident Gamma Energy (keV)	Region of Interest Energy (keV)			
	88	320	661	1115
88	(N/A)	(N/A)	(N/A)	(N/A)
320	41	(N/A)	(N/A)	(N/A)
661	12	46	(N/A)	(N/A)
1115	3	27	46	(N/A)
1836	4	8	22	49

Peak Counting Efficiency Under Discriminator:
(Normal Efficiency at Given Energy = 100)

Incident Gamma Energy (keV)	Normalized Efficiency
88	16
320	79
661	94
1115	98
1836	99

Counting Time Required Under Discriminator:
(Normal Counting Time for Conditions = 100;
counting times less than 100 represent improved sensitivity)

Desired Peak Energy (keV)	Interfering Gamma Energy (keV)			
	320	661	1115	1836
88	389	216	105	119
320	(N/A)	86	66	36
661	(N/A)	(N/A)	72	50
1115	(N/A)	(N/A)	(N/A)	71
1836	(N/A)	(N/A)	(N/A)	(N/A)

Figure 3-3. Compton Continuum for
1836-keV Incident Gammas,
Under the "Reject One-Event" Discriminator

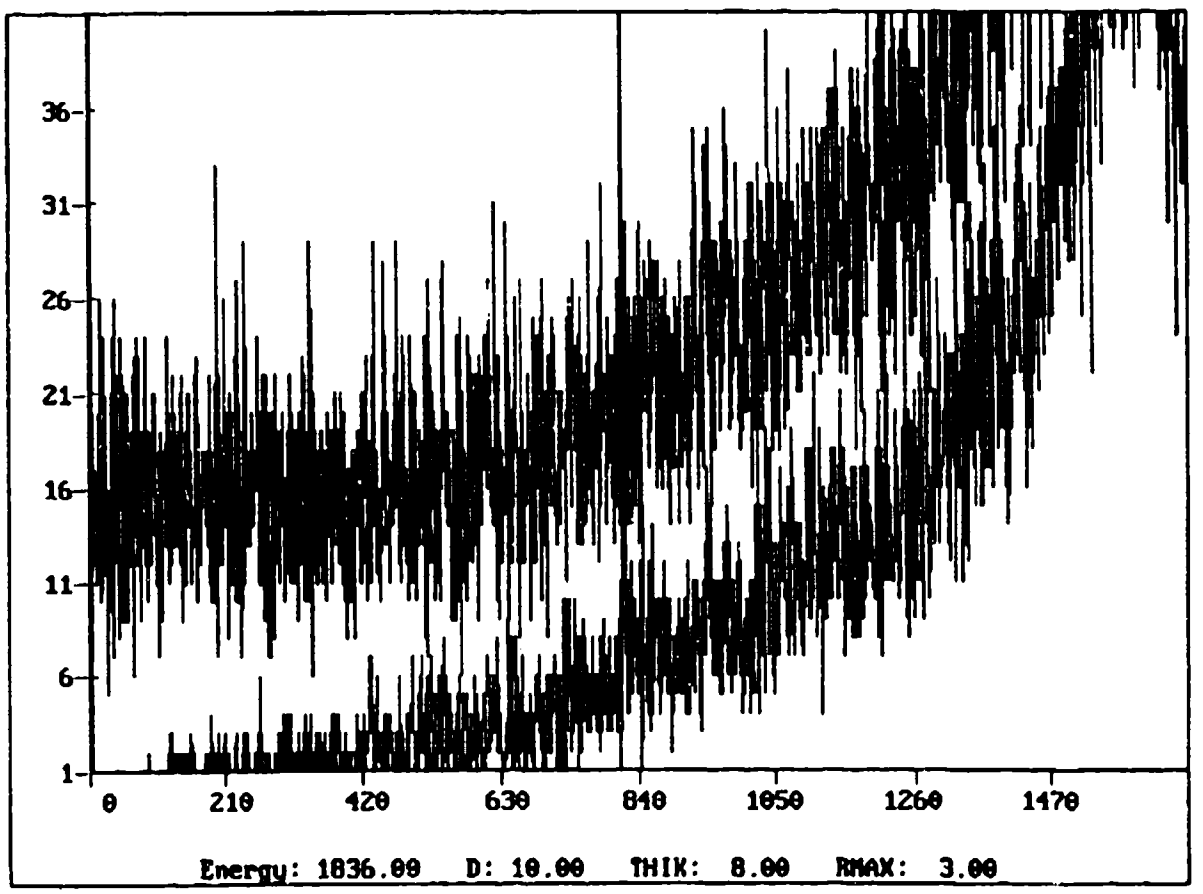

Top curve: Accept all sequences ("Normal" spectrum).
Bottom curve: Reject sequences with only one event.

Figure 3-4. Compton Continuum for
661-keV Incident Gammas,
Under the "Reject One-Event" Discriminator

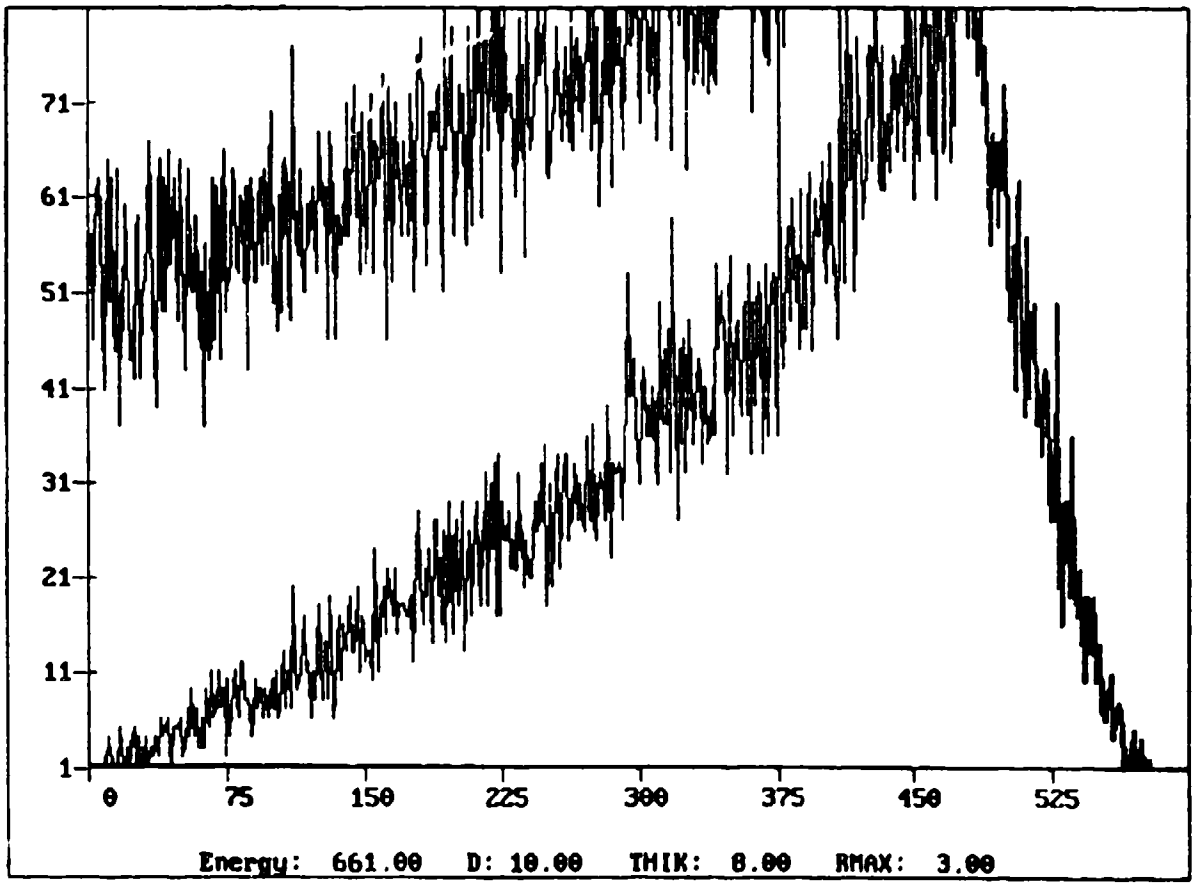

Top curve: Accept all sequences ("Normal" spectrum).
Bottom curve: Reject sequences with only one event.

3.3. Composite Discriminators

Neither event location discriminators (Section 3.1) nor event number discriminators (Section 3.2) seem to offer improvement when the same criterion is applied at all energies. This is not unreasonable, considering that the modes of gamma ray interaction change with energy. However, for each peak energy of interest, at least one criterion exists which is predicted to improve performance at that energy. Therefore, as reported below, three composite discriminators were tested in Phase I. Each composite discriminator applies different criteria to different energy ranges.

3.3.1. First Composite Discriminator (z12)

Based on the results of the single-criterion discriminators reported above, a discriminator was developed with a single different criterion applied to each of five energy ranges. The energy ranges and the criterion for each were as follows:

Energy Deposited in Sequence (keV)	Count sequence only if:
< 100	No events below 5 mm into detector
≥ 100 to < 250	No events below 15 mm into detector
≥ 250 to < 400	No events below 40 mm into detector
≥ 400 to < 900	At least 2 events in sequence
≥ 900	At least 3 events in sequence

The name for this discriminator in the project records is z12, which will be used below in referring to it.

Table 3-5 summarizes the results of applying this discriminator. Note that, unlike the single-criterion discriminators discussed above, it predicts that sensitivity would either be unaffected or improved at all energies. However, two points about this discriminator bear comment.

First, it is not optimized. The "Reject One-Event" discriminator predicts improvements at 320 keV, whereas the z12 composite does not. The knowledge gained from the "Reject One-Event" discriminator should be factored in. Furthermore, the exact energy break points were chosen somewhat arbitrarily and intuitively. Adjustment of these boundaries might improve the predicted performance.

Second, the spectrum produced by a system using this discriminator might prove challenging to conventional gamma spectroscopy software. This is because the application of different criteria to the five energy ranges produces sharp discontinuities in what is, in a normal spectrum, a relatively smooth continuum. This is illustrated by Figure 3-5, which shows both the reduction in continuum predicted for the z12 discriminator, and its sharp discontinuities at the energy break points. In practice, the break points might have to be adjusted with an eye toward avoiding energies where the peaks of important gamma emitters fall.

The preceding discussions have assumed that a general purpose spectrometer with improved sensitivity across the entire energy band is being sought. In practice many applications exist, particularly on military missions, where specific gamma emissions are to be identified and quantified in the presence of interference from higher energy gammas. In those cases, event sequence criteria and energy range break points which would maximize the sensitivity for that particular application would be applied.

Table 3-5. Results of the z12 Composite Discriminator

Continuum Level Under Discriminator:
(Normal Continuum in Region of Interest = 100)

Incident Gamma Energy (keV)	Region of Interest Energy (keV)			
	88	320	661	1115
88	(N/A)	(N/A)	(N/A)	(N/A)
320	21	(N/A)	(N/A)	(N/A)
661	23	78	(N/A)	(N/A)
1115	18	75	46	(N/A)
1836	22	72	22	17

Peak Counting Efficiency Under Discriminator:
(Normal Efficiency at Given Energy = 100)

Incident Gamma Energy (keV)	Normalized Efficiency
88	86
320	88
661	94
1115	83
1836	87

Counting Time Required Under Discriminator:
(Normal Counting Time for Conditions = 100;
counting times less than 100 represent improved sensitivity)

Desired Peak Energy (keV)	Interfering Gamma Energy (keV)			
	320	661	1115	1836
88	53	56	49	54
320	(N/A)	101	98	97
661	(N/A)	(N/A)	72	50
1115	(N/A)	(N/A)	(N/A)	49
1836	(N/A)	(N/A)	(N/A)	(N/A)

Figure 3-5. Compton Continuum for
1836-keV Incident Gammas,
Under the z12 Composite Discriminator

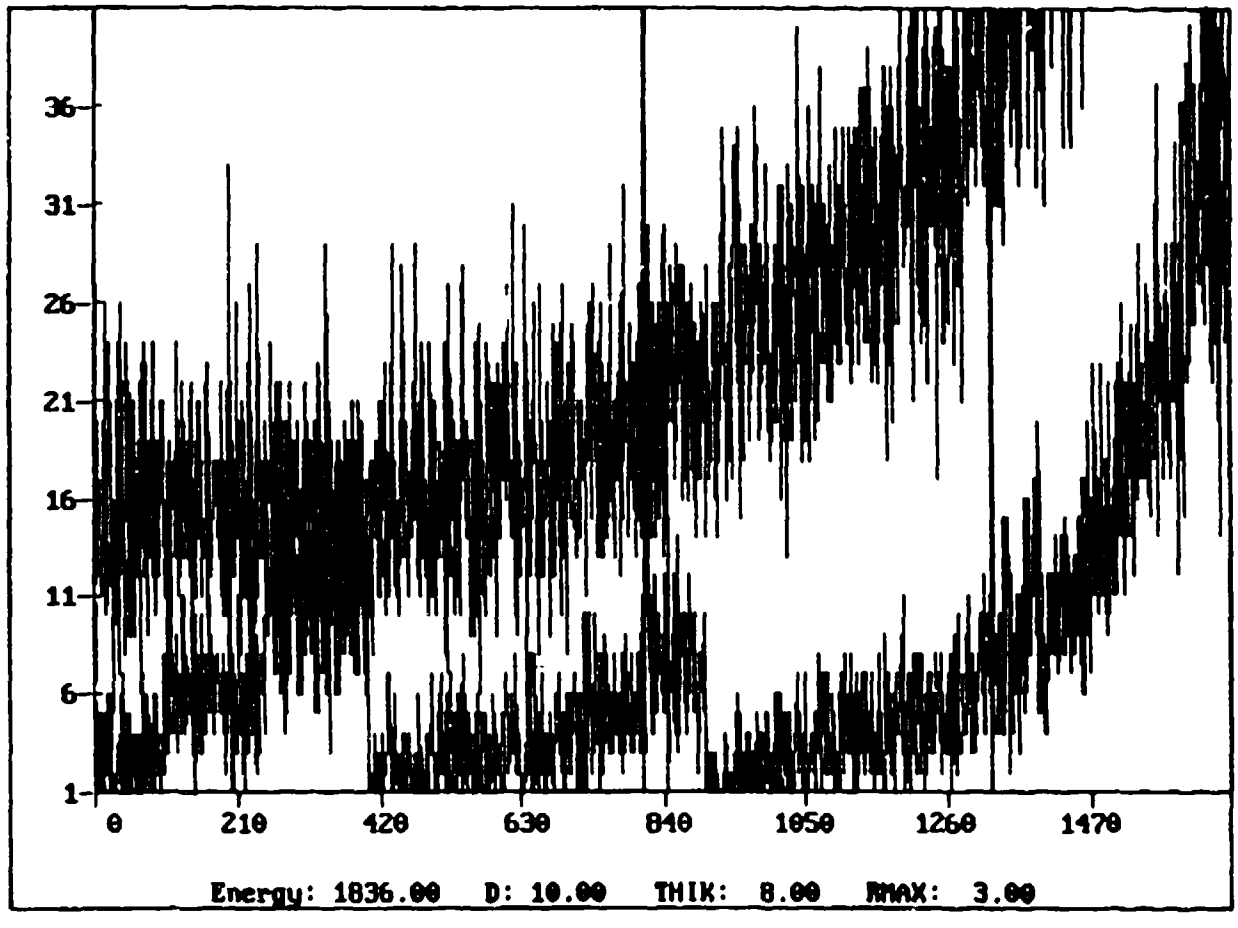

Top curve: Accept all sequences ("Normal" spectrum).
Bottom curve: z12 Composite Discriminator criteria.

3.3.2. Second Composite Discriminator (z13)

The second composite discriminator tested (z13) applied more than one criterion to the low-energy regions in the attempt to improve pred'cted performance:

Energy Deposited in Sequence (keV)	Count sequence only if:
< 100	No events below 5 mm into detector; and no more than 2 events in sequence
≥ 100 to < 200	No events below 10 mm into detector; and no more than 4 events in sequence
≥ 200 to < 400	No events below 30 mm into detector; and no more than 5 events in sequence
≥ 400 to < 900	At least 2 events in sequence
≥ 900	At least 3 events in sequence

The increased complexity did not yield an improvement in predicted performance, as Table 3-6 shows. In summary, this discriminator, while at least as good as the normal method at all energies, did no better than the simpler z12 discriminator at any energy.

Table 3-6. Results of the z13 Composite Discriminator

Continuum Level Under Discriminator:
(Normal Continuum in Region of Interest = 100)

Incident Gamma Energy (keV)	Region of Interest Energy (keV)			
	88	320	661	1115
88	(N/A)	(N/A)	(N/A)	(N/A)
320	20	(N/A)	(N/A)	(N/A)
661	23	69	(N/A)	(N/A)
1115	18	64	46	(N/A)
1836	22	59	22	17

Peak Counting Efficiency Under Discriminator:
(Normal Efficiency at Given Energy = 100)

Incident Gamma Energy (keV)	Normalized Efficiency
88	84
320	76
661	94
1115	83
1836	87

Counting Time Required Under Discriminator:
(Normal Counting Time for Conditions = 100;
counting times less than 100 represent improved sensitivity)

Desired Peak Energy (keV)	Interfering Gamma Energy (keV)			
	320	661	1115	1836
88	54	57	50	55
320	(N/A)	109	106	101
661	(N/A)	(N/A)	72	50
1115	(N/A)	(N/A)	(N/A)	49
1836	(N/A)	(N/A)	(N/A)	(N/A)

3.3.3. Third Composite Discriminator (z14)

The final attempt made in Phase I to improve on the z12 composite discriminator (called the z14 discriminator) integrated the advantages of the "Reject One-Event" discriminator into the z12 composite. This was done by extending the requirement for at least two events in the sequence down to 250 keV (effectively removing the 250-400 keV range):

Energy Deposited in Sequence (keV)	Count sequence only if:
< 100	No events below 5 mm into detector
≥ 100 to < 250	No events below 15 mm into detector
≥ 250 to < 900	At least 2 events in sequence
≥ 900	At least 3 events in sequence

The results of applying this simplified composite discriminator are presented in Table 3-7. As expected from the results of the other discriminators, the z14 composite is predicted to improve sensitivity at all energies tested: the smallest improvement is 14% for the 320-keV peak in the presence of 661-keV interference. Even for this interfering energy, however, there is a marked reduction across the whole Compton continuum, as Figure 3-6 shows.

The z14 discriminator is clearly the most successful of all the discriminators tested, despite being the least complicated of the composite discriminators tested. Nevertheless, it is not optimized: both the event depth limits (in the two lower energy brackets), and the precise energy break points (of all energy brackets) could be adjusted and might further improve predicted performance. Verification of improved performance in all energy brackets would require tests on a peak energy in the 100 - 250 keV bracket, perhaps at the energy of the Ce-144 line (134 keV).

Table 3-7. Results of the z14 Composite Discriminator

Continuum Level Under Discriminator:
(Normal Continuum in Region of Interest = 100)

Incident Gamma Energy (keV)	Region of Interest Energy (keV)			
	88	320	661	1115
88	(N/A)	(N/A)	(N/A)	(N/A)
320	21	(N/A)	(N/A)	(N/A)
661	23	46	(N/A)	(N/A)
1115	18	27	46	(N/A)
1836	22	8	22	17

Peak Counting Efficiency Under Discriminator:
(Normal Efficiency at Given Energy = 100)

Incident Gamma Energy (keV)	Normalized Efficiency
88	86
320	79
661	94
1115	83
1836	87

Counting Time Required Under Discriminator:
(Normal Counting Time for Conditions = 100;
counting times less than 100 represent improved sensitivity)

Desired Peak Energy (keV)	Interfering Gamma Energy (keV)			
	320	661	1115	1836
88	53	56	49	54
320	(N/A)	86	66	36
661	(N/A)	(N/A)	72	50
1115	(N/A)	(N/A)	(N/A)	49
1836	(N/A)	(N/A)	(N/A)	(N/A)

Figure 3-6. Compton Continuum for
661-keV Incident Gammas,
Under the z14 Composite Discriminator

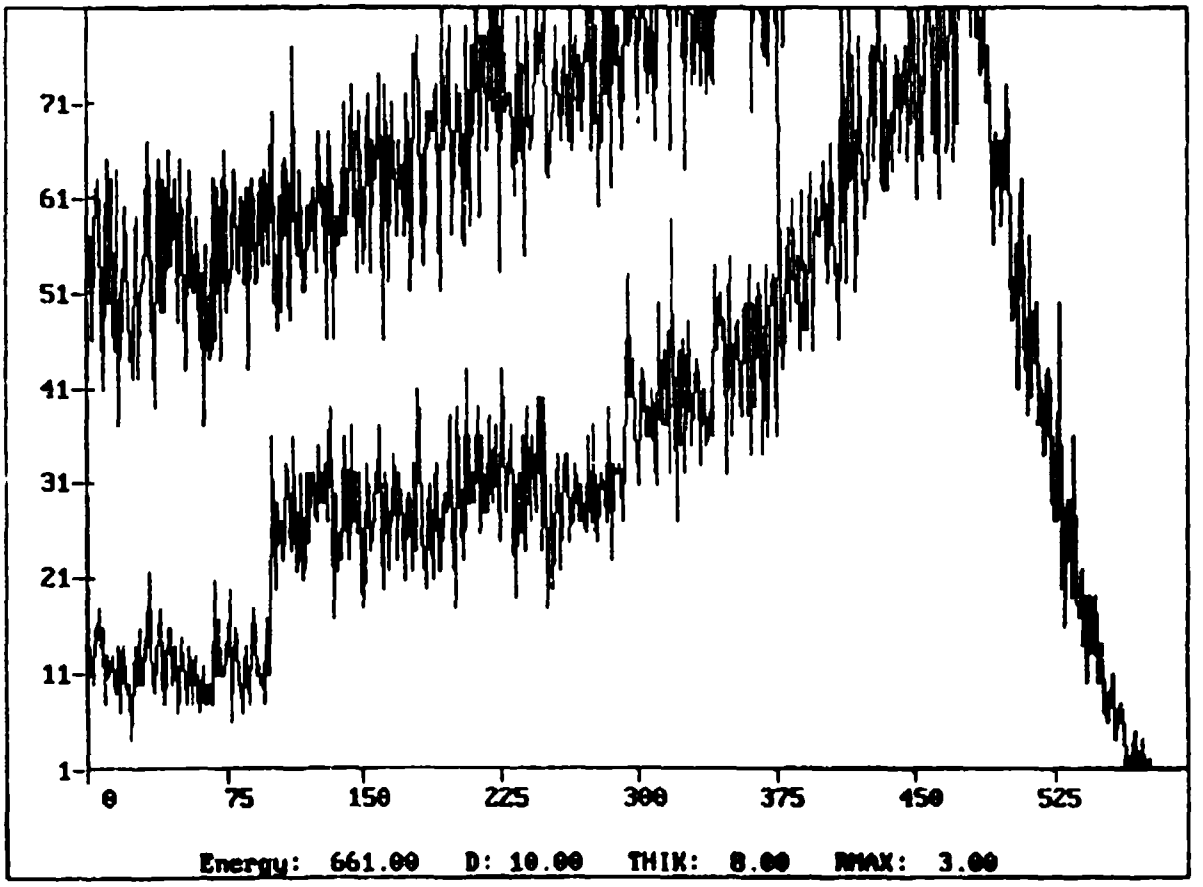

Top curve: Accept all sequences ("Normal" spectrum).
Bottom curve: z14 Composite Discriminator criteria.

3.4. Summary

Event sequence discrimination criteria were found which are predicted to suppress the Compton continuum and improve peak counting sensitivity at five peak energies in the range 88 keV to 1836 keV, when compared to the performance of a spectrometer using the same size HPGe detector and current pulse processing methods. It appears that these event sequence discrimination criteria would be effective in improving spectrometer performance at any peak energy in the given range.

Generally speaking, the most effective discrimination criteria pertain to the position of events within the detector at low deposited energies, and to the number of events in a sequence at higher deposited energies. No one criterion was found which is predicted to improve spectrometer performance at all energies in the test range, but two points should be noted. First, if only a narrow range of energies is of interest in a particular measurement, a single discriminator could probably be selected which would improve spectrometer performance compared to current methods. Second, composite discriminators which apply a different criterion to each of four or five energy brackets were shown to have improved predicted performance across the entire energy range.

Assuming that a composite discriminator could be implemented in real hardware (which is the subject of Sections 4.0 and 5.0 below), a practical problem in spectrum analysis would remain. The spectrum produced by an event sequence spectrometer using a composite discriminator would have marked changes at the edges of the energy brackets. Any full-energy peak falling on or within a few keV of one of these break points would have unpredictable size and shape, and would rest on a Compton continuum containing a sharp discontinuity. It would therefore be very difficult or impossible to analyze such a peak accurately and reproducibly. It follows that the exact energy break points would have to be chosen carefully to avoid energies where these discontinuities would pose a significant problem, and might have to be adjustable by the user within some narrow band.

4. PHYSICAL METHODS TO CHARACTERIZE EVENT SEQUENCES

The preceding sections have shown that improved spectrometer performance would be expected if it were possible to determine the number, location, or type of the energy deposition events in the detector. The question remains of whether there is reason to believe that such discrimination is possible in practice. Section 5.0 pertains to the direct determination of event types. This section discusses the plausibility of three possible methods for distinguishing the number and/or location of energy deposition events: segmented detectors, pulse shape processing, and optical event location.

4.1. Segmented Detectors

Section 1.1.4 introduced the concept of segmented detectors, referring to work that showed the potential for Compton suppression through operating the two regions of a bisected detector in the sum-coincidence mode. The block diagram of a segmented detector system in the sum-coincidence mode is shown in Figure 4-1.

Using more than two regions would clearly help in recognizing the occurrence of multiple-event sequences, with less of an efficiency penalty. For example, modeling of a 5 cm by 5 cm coaxial detector with five 1-cm thick slices has been predicted to give an efficiency 66% that of an unsegmented detector of the same size; whereas the same detector with ten 0.5-cm thick slices would have an efficiency 82% that of an unsegmented one. The predicted internal background reduction of 90%, however, would lead to an improvement by a factor of 2 to 3 in sensitivity (Va84).

Similarly, a 7 cm by 7 cm closed-ended coaxial detector has been modeled for operation in seven 1-cm slices. With a choice of coincidence summing rules that varies with the total energy deposited, such a detector would improve sensitivity by about a factor of 2 over the range 70 keV to 1 MeV (Ge84).

HPGe detectors may be fabricated from material which is either slightly n-type or slightly p-type, depending on the residual impurities. In either case, the electrical contacts must be made with surfaces that have high enough impurity levels to be good conductors. Typically, the p+ contact is made by implantation of boron ions, while the n+ contact is made through the diffusion of Li atoms. The ion-implanted electrode is always the thinner of the two, and is therefore preferred for the outside surface of the detector. Masking and photoresist methods (with chemical or plasma etching), and mechanical etching methods, are available to permit the segmentation of either type of contact (Lu84, Mi79, Pr85).

Figure 4-1. Block Diagram of a Segmented Detector Operated in the Sum-Coincidence Mode

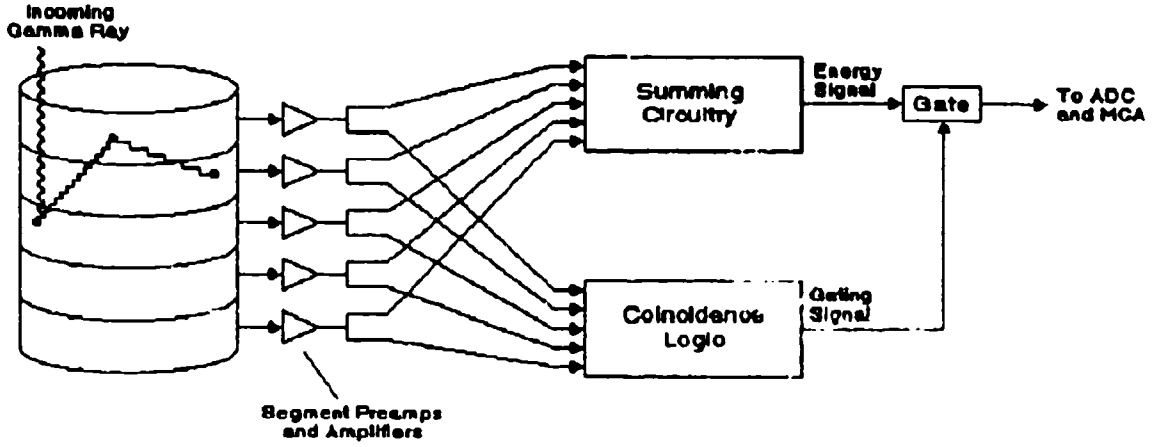

Either of the electrode surfaces of a coaxial detector (the core or the outside) could in principle be divided to produce a segmented detector. As a practical matter, the etching of the outer surface is much easier because it is more accessible (Lu84). Overall, then, the most practical characteristics of a segmented coaxial detector are an n-type bulk, with a segmented external p+ ion-implanted contact region.

Incomplete charge collection will occur in the regions near the divisions in the electrode of a segmented detector, with adverse effects on both efficiency and resolution. This was demonstrated by the sub-optimal performance of a prototype coaxial detector on which the contacts were separated by 2 mm (Ge84). However, planar arrays of large numbers of semiconductor detectors are in demand in both physics and medicine, and technology exists to reduce the spacing between contacts to the 150-200 μm (He89, Mi79, Pr85).

On a related topic, it should also be noted that spatial resolution as small as 0.5 mm has been measured in a planar detector of unique design, fabricated from specially selected germanium. This detector permits the determination of electron drift time (the time required for the electrons to migrate from the interaction site to the anode), which is related to the position of the interaction site. An impurity gradient in the germanium allows the required electric field to be produced without segmentation of the external electrodes. However, the drift times are so long (on the order of 1 μsec for a detector dimension of about 3 cm) that count rates must be kept fairly low (Lu85).

In summary, both calculations and prototype measurements agree on the likely sensitivity benefits of a properly-operated segmented detector. The technology is in hand to permit the construction of a coaxial detectors with almost any desired electrode width or spacing. There appears to be nothing to prohibit the application of segmented detector methods to laboratory measurements.

4.2. Pulse Shape Processing

Segmented detectors can certainly be built that are adequate for spectrometric purposes. However, segmentation has its drawbacks in discriminating between multiple- and single-event sequences, drawbacks which are separate from the difficulties inherent in the manufacture of the detector crystal. In particular, for multiple-event sequences to be recognized, the events must occur in different segments. This means that the more segments there are, the greater should be the sensitivity improvement. But each segment requires its own separate pulse processing circuitry, which adds to the size and complexity of the assembled system. Furthermore, the energy calibration of each segment must be known separately, if one is to apply discrimination criteria based on amounts of energy deposited in separate segments (rather than simply the occurrence of events in single or multiple segments).

For the above reasons, it would be desirable to have a method to tell how widely dispersed in the crystal the event sites were, without the resort to detector segmentation. One such method is pulse shape processing: the examination of the timing characteristics of the leading edge of the preamplifier output signal pulses.

It is well known in experimental physics that detector output pulse rise time is not constant, but is dependent on the location of the site where the energy deposition created the charge carrier pairs. The interest of the physicists is to compensate for this variability, to permit accurate timing for comparison of results in different detectors, but their studies have established the existence of timing effects which may be useful in event sequence analysis for the suppression of partial-energy absorption sequences.

White (Wh74) lists the following factors affecting the output pulse shape:

a. the electric field as a function of position inside the sensitive volume of the detector;
b. the electron and hole mobilities in the detector material, which are functions of the electric field and temperature; and
c. the initial distribution of charge carriers in the detector volume, which is a function of the energy and type of incident radiation.

Even in a simple planar detector, in which the electric field should theoretically be constant throughout, there are edge effects and other areas of low electric field which may produce appreciable effects on the leading edge shapes of

germanium detector pulses (Be72, Ka82, Mo86). But in a planar detector whose electrode design has been modified to maximize efficiency, the convoluted electrical field shape is said to make the device useless to physicists for timing experiments (Va87). In a detector material such as mercuric iodide, in which (unlike HPGe) the mobilities of holes and electrons differ considerably, the effect is even more pronounced (Be86). In all cases, energy deposition events occurring near one or the other electrode produce relatively slow rise time pulses, compared to pulses from events occurring near the center of the detector.

A coaxial detector has an unavoidable 1/r variation in electric field due to its cylindrical geometry, even without the added complexity of the distorted electric field in a closed-end geometry. This suggests that it should be possible to tell something about the interaction location from the shape of the leading edge, which is indeed the case.

White and McDonald (Wh74) provide theoretical equations for pulse shape calculations in a true coaxial detector with charge created at a single point, under the assumption of equal electron and hole mobilities, and ignoring any space charge effects. They present calculations for a detector typical of their work, which were modified in the present research to more nearly represent present-day detectors. The detector characteristics assumed for the calculations presented in Figure 4-2 were the following:

Parameter	Value
Detector Outside Radius	3.5 cm
Detector Core Radius	0.3 cm
Applied Voltage	4000 V
Carrier Mobility (at 77 K)	39000 $cm^2/(V\ sec)$

These parameters lead to a maximum charge collection time (for charges produced near either electrode) of about 97 nsec. The predicted rise times are about half those reported by other workers, who used a different formulation and based their calculations on a smaller detector (Ra82). Rise times of 50-200 nsec, with variations in the few tens of nanoseconds, are apparently realistic.

The leading edge slope or fraction of final height at a given time, is clearly a complex function of the distance from the detector center to the interaction site, even ignoring the closed-end region. The rise time variability offers the potential to distinguish between single- and multiple-event sequences because multiple-event sequences produce charge at several points which will in general have different electric fields. Their pulse shapes should be more typical of the whole detector sensitive volume than of the region near either

electrode. Furthermore, to the extent that an event discrimination criterion of this kind selects for events in the bulk of the detector, and away from the outside edge, it will favor full-energy sequences (see Section 2.3.2).

The question now arises of whether there is established technology for measuring differences in rise times on the order of a few tens of nanoseconds. The general answer is that sub-nanosecond timing is commonplace in physics. Specifically, it should be recalled that the observed effects of these rise time variations were what stimulated interest in them. Indeed, several researchers have published results of rise time measurements that are in broad agreement with the above discussion (Be72, Ra82, Va87, Wh74). An amplifier design was reported recently which handles certain pileup problems, preserves the original pulse size, and makes a reproducible translation between input rise time and output rise time (Ma87). Therefore, the expected differences in detector pulse shape due to interaction locations should be readily measurable in the laboratory.

Figure 4-2. Computed Leading Edge Shapes for Coaxial Detector Output Pulses

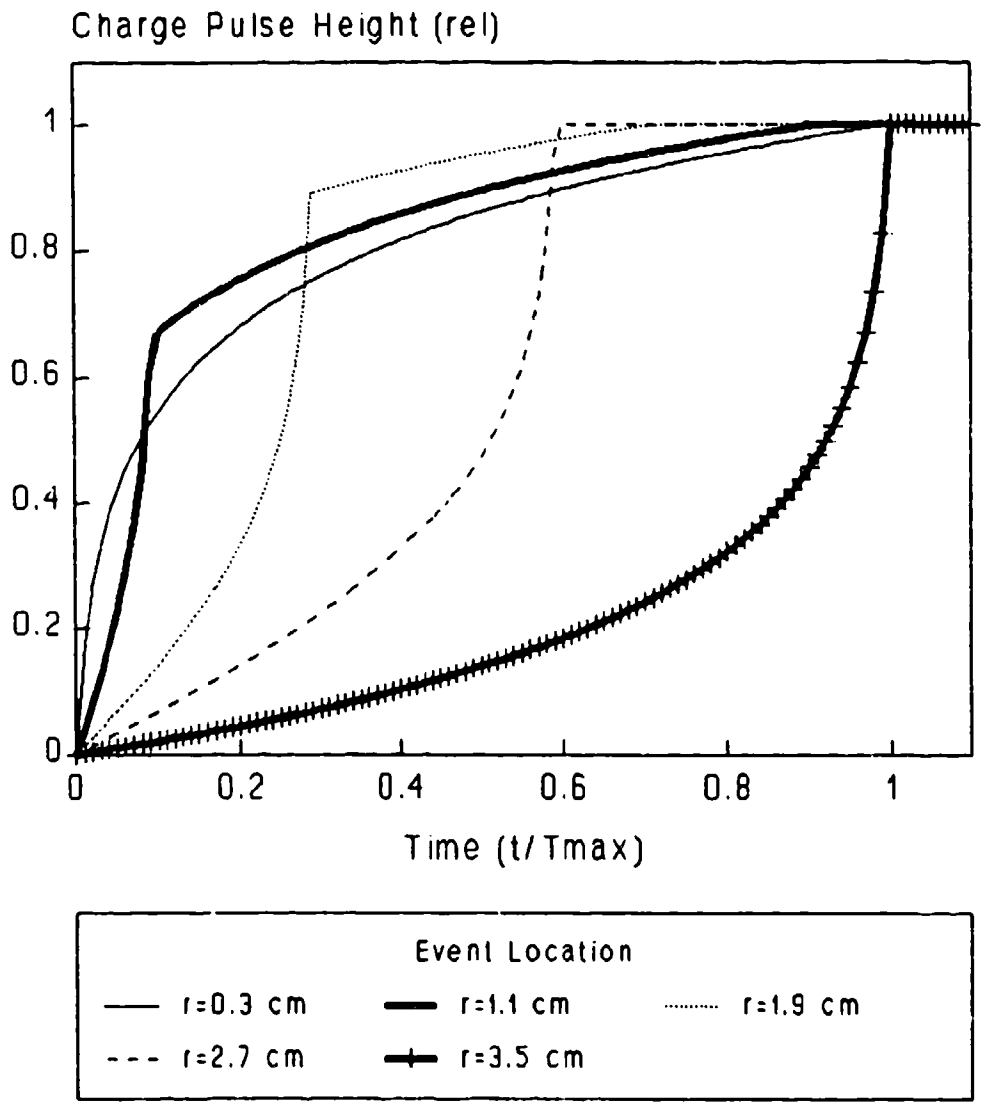

Note: Tmax =96 nsec

4.3. Optical Location of Events

In addition to the segmented region and pulse rise time methods discussed in Sections 4.1 and 4.2, there is an additional possible method for locating interaction events within the HPGe crystal: detection of radiative events associated with the charge pairs that carry the electronic signal. Optical methods must be classified as speculative at this point, and were not investigated in detail during Phase I. However, the technical monitors of the Phase I work have intimated that research exists on this subject which might be made available during a Phase II project. The following may then be viewed as suggestive facts regarding optical event location methods.

First, it should be noted that the electronic signal is carried by electrons and holes. Where electrons and holes exist in a solid lattice, the potential is present for radiative de-excitation of the pairs, which might produce optical photons detectable outside the lattice. However, in high-purity crystals of near-perfect structure, operated with high electric field, recombination is minimized. This is a basic in detector design. Therefore, the extent of such radiative de-excitations in HPGe detectors, though not determined in this research, is expected to be small.

Another possibility for radiative transitions in HPGe is charge trapping, a known effect whose influence on the shape of the charge pulses is said to be compensable (e.g., Si89). But the very fact that trapped charges affect pulse shape implies that they are ultimately collected, so their ultimate de-excitation cannot be a radiative recombination; it must be a charge recombination at an electrode. This does not preclude the possibility that the original trapping event itself is accompanied by a radiative transition. Photons from the original trapping event would be far below the 0.75 eV width of the germanium band gap at 0 K, perhaps 0.01 eV. HPGe might or might not be transparent at these wavelengths in the infrared (on the order of 0.01 mm to 1 mm), but it is known to be transparent enough for use as an optical filter in the 0.002 mm to 0.02 mm range (Gr68).

A considerable literature exists on induced photon emissions from germanium (e.g., Ch84, Ko85, Ko86). In general, such emissions have been produced under conditions similar to the following: a) the presence of crossed electric and magnetic fields, with the electric field pulsed at 2 to 8 Hz; b) electric field strengths on the order of 1 to 2 kV/cm; and c) dopant levels on the order of 1 E+13 to 20 E+13 per cm^3. The induced emissions are in the 0.05 mm to 0.25 mm range, and escape the germanium crystals through pathlengths as long as 5 cm.

It is not immediately obvious how comparable emissions might occur spontaneously in an HPGe detector. In particular, although the applied electric field in an HPGe detector is comparable to the 1 to 2 kV/cm, it is steady-state and not pulsed. In addition, residual impurity levels in HPGe are three to four orders of magnitude less than in the specimens used in the experiments cited above, but the dopant plays a crucial role in the induced emissions. Despite these differences in the bulk conditions in the two kinds of experiments, the transient and local conditions in the immediate vicinity of a charge deposition site in an HPGe detector might possibly support some radiative emissions. Collaboration with specialists in solid state optical transitions during the Phase II effort would be used to clarify this question.

It should be noted that, in general, radiative transitions from recombination or trapping could occur at millimeters or centimeters away from the site where the charge carriers were originally created: either one could happen anywhere between the point of creation and the collecting electrode. Therefore, the precision of the location information that could be inferred from them might be rather limited. However, if radiative transitions were dependent on the local and transient conditions in the vicinity of the charge pair creation site, the location inference might be much more reliable. This, then, would seem to be the more promising line of inquiry for Phase II.

4.4. References

Be72 Bengtson, B.; Moszynski, M. "Subnanosecond Timing with a Planar Ge(Li) Detector." Nucl. Instrum. and Meth. 100: 293-300; 1972.

Be86 Beyerle, A.; Gerrish, V.; Hull, K. "Parallel Pulse Processing for Mercuric Iodide Gamma-Ray Detectors." Nucl. Instrum. and Meth. in Phys. Res. A242: 443-449; 1986.

Ge84 Gehrels, N.; Cline, T.L.; Teegarden, B.J.; Tueller, J.; Leventhal, M.; MacCallum, C.J.; Hewka, P.V.; Ryge, P. "The Development of a Segmented N-Type Germanium Detector, and Its Application to Astronomical Gamma-Ray Spectroscopy." IEEE Trans. Nuc. Sci. NS-31 (1): 307-311; 1984.

He89 Heijne, E.H.M.; Jarron, P. "Development of Silicon Pixel Detectors: An Introduction." Nucl. Instrum. and Meth. in Phys. Res. A279: 467-471; 1989.

Ka82 Kawade, K.; Battistuzzi, G.; Lawin, H.; Sistemich, K. "On the Timing Properties of Ge Detectors." Nucl. Instrum. and Meth. 200: 583-585; 1982.

Lu84 Luke, P.N. "Gold-Mask Technique for Fabricating Segmented-Electrode Germanium Detectors." IEEE Trans. Nuc. Sci. NS-31 (1): 307-311; 1984.

Lu85 Luke, P.N.; Madden, N.W.; Goulding, F.S. "Germanium Detectors with a Built-In Transverse Drift Field." IEEE Trans. Nuc. Sci. NS-32 (1): 457-462; 1985.

Ma87 MacArthur, D.W.; Morgado, R.E. "Fast Pulse-Shaping Amplifier." Nucl. Instrum. and Meth. in Phys. Res. A262: 378-384; 1987.

Mi79 Miller, D.; Schlosser, P.; Deutchman, A.; Steidley, J.; Hunter, W.; Gerber, M.; Profant, R.; Yocum, M.; Hyland, R. "A Multi-Detector Germanium Gamma Ray Camera." IEEE Trans. Nuc. Sci. NS-26 (1): 603-609; 1979.

Mo86 Morozov, V.S.; Stegailov, V.I.; Yashin, S.N.; Zinov, V.G. "Effect Produced by the Charge Collection Time Upon the Time and Energy Resolution of Semiconductor Detectors." Nucl. Instrum. and Meth. in Phys. Res. A248: 405-415; 1986.

Pr85 Protic, D.; Riepe, G. "Position-Sensitive Germanium Detectors," IEEE Trans. Nuc. Sci. NS-32 (1): 553-555; 1985.

Ra82 Raudorf, T.W.; Bedwell, M.O.; Paulus, T.J. "Pulse Shape and Rise Time Distribution Calculations for HPGe Coaxial Detectors." IEEE Trans. Nuc. Sci. NS-29 (1): 764-768; 1982.

Va84 Varnell, L.S.; Ling, J.C.; Mahoney, W.A.; Jacobson, A.S.; Pehl, R.H.; Goulding, F.S.; Landis, D.A.; Luke, P.N.; Madden, N.W. "A Position-Sensitive Germanium Detector for Gamma-Ray Astronomy." IEEE Trans. Nuc. Sci. NS-31 (1): 300-306; 1984.

Va87 Van Duppen, P.; Duhamel, P.; Vanhorrenbeeck, J. "Timing Properties of a 'LEGE'-Type (Low Energy Germanium) Detector." Nucl. Instrum. and Meth. in Phys. Res. A254: 401-405; 1987.

Wh74 White, D.C.S.; McDonald, W.J. "Recent Developments in Subnanosecond Timing with Coaxial Ge(Li) Detectors." Nucl. Instrum. and Meth. 115: 1-11; 1974.

5. DISTINGUISHING BETWEEN COMPTON AND PHOTOELECTRIC EVENTS

5.1. Significance of Compton / Photoelectric Discrimination

The discussions of the previous sections have shown that event sequence analysis techniques appear to offer improved sensitivities for measuring certain combinations of primary and interference gamma rays. Additionally, the application of simultaneous criteria on event location, energy deposition, and the number of events was shown to give predicted performance improvement over the gamma energy range of 50 keV to 2 MeV. In all cases, criteria were selected and applied which favor full energy event sequence over sequences which contribute non-informative background counts.

Based on the previous theoretical and Monte Carlo analyses of gamma interaction sequences, it is obvious that the event sequence criterion which would give maximum sensitivity improvement would be the ability to accept only event sequences which end in a photoelectric event. If this criterion could be imposed, all of the full energy peak counts would be accepted, while all of the background counts from Compton escape events in the detector would be eliminated.

Since Compton escape events contribute most of the baseline counts in typical spectra, the remaining spectrum would consist primarily of full energy peaks on a flat, very low level background continuum. The improvement in detection sensitivity is obvious, since the full energy peak efficiency (ϵ) would remain unchanged, while the baseline count (B) from Compton escape events would be eliminated. If realizable, this improvement would provide a major breakthrough applicable to military, nuclear research, nuclear power, and environmental monitoring needs.

In this section, the concept of distinguishing between photoelectric and Compton interaction events in a germanium detector will be examined briefly. In particular, the two scattering interaction mechanisms will be reviewed to see if characteristic differences might exist in the scattering or de-excitation mechanisms, and if a means can be found which might allow the different mechanisms to be identified in an operating detector.

It is recognized that pursuit of this concept is a high risk, high return portion of the study. Although the separation of Compton and photoelectric events in a semiconductor detector has not been accomplished (nor attempted, to our knowledge), the revolutionary performance improvement offered by this approach would seem to warrant further study if plausible approaches can be identified.

5.2. Differences in Compton and Photoelectric Interactions

The ability to distinguish between Compton and photoelectric interaction events requires that some "signature" phenomenon be identified which can be observed external to the detector. Such a signature phenomenon might be a unique emission or de-excitation related to the nuclear interaction, the atomic restructuring, the semiconductor lattice effects, or the charge distribution. In the following paragraphs, Compton and photoelectric interactions will be reviewed briefly to identify differences which might serve as the basis for distinguishing between the two event types in an operating detector.

In Appendix A of this report, the common gamma interaction mechanisms are discussed in some detail. It is noted that Compton scattering is an interaction between the electromagnetic field of the photon and any atomic electron in the lattice. Momentum conservation is between the electron and the scattered photon, and the scattered photon is polarized. The recoil electron direction is predominantly forward, and is never greater than 90° with respect to the incident photon direction.

Photoelectric interaction involves the total absorption of the photon energy in an interaction of the electromagnetic field of the incident photon and a tightly bound (inner shell) electron. Because an inner shell electron is ejected by this interaction, X-rays and Auger electrons are produced during the atomic energy level repopulation process. Momentum conservation must occur between the ejected electron, the recoiling nucleus, and phonon effects in the lattice, since no photon is produced in a photoelectric interaction. The ejected electron direction can have any angle, and is predominantly sideways at low photon energies.

For both photoelectric and Compton interactions, the primary product of the interaction and subsequent slowing down of the ejected electron is a localized volume of free charge carriers in the lattice. This "plasma" of electrons and holes has initial dimensions of 1-2 mm, except for cases where the electron slowing down process occurs along preferred channeling directions in the lattice (To69, De64).

The plasma is probably very similar for a Compton or a photoelectric interaction which releases the same energy in a single interaction. Some differences in the shape and orientation of the plasma volume might exist due to differences in the energy and momentum redistribution processes. Since the photoelectric interaction involves strong coupling with the atom and the lattice, it clearly would have a different distribution of X-rays, phonon interactions, and optical transitions.

Our search of the literature showed limited previous work in determining the nature of gamma interaction products in a semiconductor lattice, and no theoretical or experimental work on distinguishing Compton and photoelectric interaction events. Several groups reported plasma and charge collection models, but these works were directed to defining charge cclllection phenomena rather than to defining the products of the interaction process (To69, Ra82).

Thus, physical differences can be identified between the Compton and photoelectric de-excitation processes in a semiconductor lattice. It is yet to be determined if these differences can be observed external to the detector in a manner which would allow the separation of Compton and photoelectric interactions.

5.3. Possible Methods for Separating Event Types

Possible approaches to distinguish between Compton and photoelectric interactions in an operating detector would be to use differences in the resulting plasma effects, the optical transitions, the phonon interactions, or the X-rays or Auger electrons. With each of these phenomena, the difficult task is to devise a means to observe and characterize the effect external to the detector volume. Each of the phenomena is a local event internal to the detector volume, and the products of the phenomenon are quickly reabsorbed within the semiconductor lattice.

One potential method of characterizing the interaction products involves using the oscillatory properties of the plasma. During the past decade, various groups have predicted and experimentally measured oscillatory phenomena related to electron-hole plasmas in germanium. These experiments have confirmed emissions from very low frequency electrical oscillations, to laser operation in the far infrared (FIR) region. In several cases, the dopant concentration and temperature were similar to those common to operating germanium detectors.

In 1979, a Russian group predicted spontaneous FIR emission from germanium in crossed electrical and magnetic fields (An79), which was experimentally verified by another Russian group in 1981 (Iv81). A Japanese group confirmed the spontaneous FIR emissions, but expressed skepticism that laser operation in germainum could be achieved (Ko82). In 1984, the Russian team demonstrated laser operation in germanium (An84), which was subsequently confirmed by the Japanese group (Ko85).

During this same period, research groups in the United States and elsewhere showed that lower frequency spontaneous oscillations are generated in germanium under electric, or perpendicular electric and magnetic fields. The observed oscillations ranged from the 100 Hz range (Te83), to 113 kHz (He84), and were stimulated by light pulses, AC sources (Bu86), or spontaneous emission (Sc86). One group used femtosecond laser pulses to generate a dense electron-hole plasma in germanium at 77° K (Hu85). The observed oscillations have in common that they result from the dynamic behavior of the electron hole plasma, and from impact ionization phenomena in the dispersal of the carriers.

These theoretical and experimental confirmations of oscillatory behavior resulting from the presence of a localized electron-hole plasma suggest that similar phenomena might be produced in a Ge detector. Within the active volume of an operating Ge detector, the energy loss by an incident photon in either a Compton or photoelectric interaction goes primarily into the generation of a dense electron-hole plasma at the location of the interaction.

The oscillatory output would be characteristic of the plasma and of the lattice, and might show differences related to the characteristic plasma and de-excitations in the Ge lattice corresponding to each interaction type. A waveform analysis of spontaneous emissions following Compton and photoelectric interactions would provide an interesting test of possible "signature" behavior for each event type.

Such AC behavior is not presently observed in conventional Ge detector systems because charge collection and pulse processing circuits are designed to suppress oscillatory electrical signals. New front-end electronics to collect and process the AC signals could readily be designed and fabricated. Live time processing and analysis of output signals are now more practical based on high density analog and microprocessor chip developments of the past few years. One research team recently reported the fabrication of a JFET preamplifier directly on the semiconductor volume of a silicon detector (Ra88). The reduced capacitance and noise of such a closely coupled preamp provide resolution and high frequency capabilities not previously achievable.

Our research did not find experimental attempts to measure optical (FIR) emissions from semiconductor radiation detectors, although the military sponsor indicated that related topics may be under investigation in other areas. An analysis of the FIR signal likely would also show distinctive patterns based on the nature of the electron-hole plasma.

Several of the experimental systems used perpendicular electric and magnetic fields within the germanium volume. If a promising discrimination technique requiring a magnetic field is found, it would be necessary to find a practical means to establish a magnetic field within a Ge detector.

5.4. Conclusions on Compton/PE Discrimination

In this section, it has been shown that differences exist between the products of Compton and photoelectric interactions in the germanium lattice. It also has been shown that recent research into dense electron-hole plasma in germanium has demonstrated that electrical or optical signals related to the behavior of the plasma can be measured outside of a germanium sample.

Our simple review does not establish that similar signals can be observed in an operating Ge detector, nor that the signals contain information which would allow the discrimination of Compton and photoelectric events in the detector volume. The review does appear to support the pursuit of AC phenomena, on an empirical basis, as a reasonable means to evaluate techniques for distinguishing between event types or sequences in semiconductor detectors.

This high risk / high return topic represents an area for further study in which neither the technical basis nor the state of development of electronics were available a decade ago.

5.5. References

An79 Andronov, A.A.; Kozlov, V.A.; Mazov, L.S.; Shastin, V.N. Sov. Phys. - JETP Lett. 30: 551; 1979.

An84 Andronov, A.A.; Zverev, I.V.; Kozlov, V.A.; Nozdrin, Yu.V.; Pavlov, S.A.; Shastin, V. N. Sov. Phys. - JETP Lett. 40: 804; 1984.

Bu86 Bumeliene, S.B.; Pozhela, Yu.K.; Pyragas, K.A.; Tamasevicius, A.N. "Subharmonic Bifurcations and Chaotic Response in n-Ge:Ni Periodically Driven by an Electric Field." In: Proc. 18th Intl. Conf. Phys. Semicond. Stockholm: World Scientific; 1986: 1563-1566.

De64 Dearnaley, G. IEEE Trans. Nuc. Sci. NS-11(3): 249; 1964.

He84 Held, G.A.; Jefferies, C.; Haller, E.E. "Observation of Chaotic Behavior in an Elecrton Hole Plasma in Ge." Phys. Rev. Lett. 52: 1037-1040; 1984.

Hu85 Hulin, D.; Combescot, M.; Bok, J.; Migus, A.; Antonetti, A.; Vinet, J.Y. "Dissipation Processes in Semiconductors During Irradiation with Femtosecond Pulses." Proc. 17th Intl. Conf. Phys. Semicond.: 1275-1279; 1985.

Iv81 Ivanov, Yu.L. Sov. Phys. - JEPT Lett. 34: 515; 1981.

Ko82 Komiyama, S. Phys. Rev. Lett. 48: 271; 1982.

Ko85 Komiyama, S.; Iizuka, N.; Akasaka, Y. "Evidence for Induced Far-infrared Emission from p-Ge in Crossed Electric and Magnetic Fields." Appl. Phys. Lett. 47: 958; 1985.

Ra88 Radeka, V.; Rehak, P.; Rescia, S.; Gatti, E.; Longoni, A.; Sampietro, M.; Holl, P.; Struder, L.; Kemmer, J. "Design of a Charge sensitive Preamplifier on High Resistivity Silicon." IEEE Trans. Nuc. Sci. 35(1): 155-159; 1988.

Sc86 Scholl, E.; "Competing Mechanisms for Complex Chaotic Dynamics in Hot Carriers." In: Proc. 18th Intl. Conf. Phys. Semicond. Stockholm: World Scientific; 1986: 1555-1558.

Te83 Teitsworth, S.W.; Westervelt, R.M. "Nonlinear Oscillations and Chaos in Electrical Breakdown in Ge." Phys. Rev. Lett. 51: 825-828; 1983.

To69 Tove, P. A.; Seibt, W. "Plasma Effects in Semiconductor Detectors." Semiconductor Nuclear Particle Detectors and Circuits. Washington, D.C.: National Academy of Sciences; Publication 1593; 1969.

6. CONCLUSIONS FOR PHASE I

A strong interest exists in improving sensitivities for gamma ray spectrometry using semiconductor detectors as evidenced by the ongoing efforts for improved performance in fields of basic research, applied nuclear monitoring, and military and space applications. This Phase I study investigated performance improvements offered by dynamic analysis of individual scattering sequences as made possible by recent advancements in detector fabrication and microprocessor technology.

Based on the results of this Phase I study, several conclusions are offered:

1. Methods which have provided steady improvements in detection sensitivity during the past two decades have reached a point of diminishing returns where subsequent improvements will be incremental, and come at a very high cost. In particular, increases in semiconductor crystal size which were responsible for the most significant performance improvements are now bounded by significant physical and cost constraints.

2. Based on the Monte Carlo predictions of this study and of related experimental results, event sequence analysis of scattering sequences in semiconductor detectors was shown to provide significant sensitivity improvements for measuring certain gamma ray emissions in the presence of background from higher energy gamma rays. Selection criteria were based on interaction locations, number of interactions, or energy deposited. Simultaneous application of selected event sequence criteria were shown to produce sensitivity improvements for an incident gamma ray energy range of 50 - 2000 keV.

3. The use of established segmented region detector technology and/or rise time measurement methods appears to offer a practical means to implement event sequence analysis on an operating semiconductor detector. Optical emission detection related to gamma ray interactions is a possible, but less established method.

4. The ability to distinguish event sequences ending in Compton scattering from those ending in photoelectric absorption would provide a revolutionary improvement in detector performance. Certain research findings in semiconductor plasma behavior during the past decade may offer a means to differentiate between known physical differences in the two interaction mechanisms. This area is recognized as a secondary, more speculative area with less probability of success than other event sequence methods, but with very significant benefits, if achieved.

7. PRELIMINARY PLANS FOR PHASE II

The Phase I project used a Monte Carlo model to identify areas in which event sequence analysis techniques are predicted to offer improved detection sensitivities over conventional gamma spectroscopy methods. Signal processing methods were identified which appear to allow practical operation of a germanium detector in an event sequence analysis mode.

The Phase II effort would develop the means to apply event sequence processing to specific nuclear measurement needs, and would experimentally verify the actual performance attainable for specific applications. Major steps involved in the effort are as follows:

1. Extend the Monte Carlo Model to allow the specification of detector geometries and operating conditions for applying event sequence processing to practical measurement situations.

   The existing Monte Carlo model would be expanded to include certain effects necessary to predict performance in actual situations. This expanded model could be used to specify beneficial event sequence analyses for existing detectors, or to predict detector configurations which would offer improved sensitivity under given measurement conditions.

2. Set up a measurement system which would allow testing of various event sequence analysis criteria on operating semiconductor detectors.

   The test system would allow operation of segmented detectors, or would permit pulse rise time and waveform analysis of detector output pulses. Optical signal measurements would be implemented if justified by further evaluation. Collimated gamma ray beams of selected energies from low intensity radionuclide sources would be used to test position sensing criteria and general performance of detectors.

3. Select and evaluate the performance of event sequence processing spectrometers for specified measurement needs.

   For applications suggested by SDI program needs, or for an actual gamma spectroscopy monitoring application need, event sequence processing spectrometers would be designed and optimize with the Monte Carlo model, then assembled and tested with the measurement system. This evaluation would be the "proof of the pudding"; it would determine real performance in an actual measurement situation.

4. Use the detector test system to perform preliminary experiments on discriminating between Compton and photoelectric interactions in a detector.

   The fast electronics processing system used for the pulse shape discrimination would be used to look for characteristic AC emissions for Compton and for photoelectric interaction events in the detector. This would be a brief empirical study to determine if discrimination methods worthy of further study could be identified.

At the conclusion of the Phase II effort, the feasibility of practical event sequence processing spectrometers would be established. Sufficient capability would exist to specify gamma ray spectrometer designs and operating conditions for military missions, research systems, or civilian radiation monitoring applications. The commercial potential of such spectrometers is significant, and has already generated interest among manufacturers of germanium detectors for gamma ray spectroscopy.

APPENDIX A

Basic Physics of Gamma Ray Interactions with Matter

A.1. CLASSIFICATION OF PROCESSES

Following Fano (Fa53), it is possible to list four (4) types of interactions of electromagnetic radiation with atoms, and three (3) outcomes of such interactions.

A.1.1. Interactions. The four interactions are:

I. Direct electromagnetic interaction with atomic electrons. The moving photon causes an oscillating electric force on the charge of the electron, and a smaller magnetic torque.

II. Direct electromagnetic interaction with nucleons. The photon causes an oscillating electric force on the protons (only) because of their charge, and a smaller magnetic torque on both the neutrons and protons.

III. Interaction with electric field surrounding charged particles (electrons or nucleons). The photon induces an electromagnetic current in space in which there is an electrostatic field. This current is associated with the production of electron-positron pairs.

IV. Interaction with the meson field surrounding nucleons. The photon induces an electromagnetic current in space in which there is a meson field. This current is associated with the production of mesons.

A.1.2. Outcomes. For the photon, the four possible outcomes are:

A. Complete absorption. The photon transfers all of its energy to the system, and disappears.

B. Elastic scattering. The photon is deflected, but the interacting system (atom) recoils as a whole, gaining no energy. The photon therefore gives up no energy.

C. Inelastic scattering. The photon is deflected, and one or more parts of the interacting atom recoil with respect to the others, increasing the energy of the interacting system. The photon therefore gives up some energy to the medium.

A.1.3. Possible processes. Since there are four possible interactions and three possible outcomes, there are (at least theoretically) 4 x 3 = 12 possible gamma interaction processes. Many are very improbable and some have not been observed experimentally. At radionuclide energies (i.e., ~0.1 to ~6 MeV), and for the purposes of detecting the radiation, the twelve possibilities distill down to three:

IA. Photoelectric effect. The photon interacts with a bound electron and disappears. The electron is ejected from the atom with the entire energy of the photon, minus the electron binding energy.

IC. Compton scattering. The photon interacts with an electron which behaves as if it were free. The electron flies off with a considerable fraction of the photon energy (but not all), and the photon is deflected through an angle which depends on the fraction of the energy imparted to the electron.

IIIA. Pair production. A photon of energy > $2m_e$ (i.e., > 1.022 MeV) disappears in neighborhood of a nucleus (or sometimes in the neighborhood of an orbital electron), and an electron-positron pair appears. Their total kinetic energy is the remainder of the photon energy, after the deduction of the $2m_e$ required to create the pair.

Note that Rayleigh scattering (IB), though usually thought of as quite improbable at common energies, is actually only one or two orders of magnitude less likely than Compton scattering, even at energies as high as 0.1 MeV. However, since it is an elastic interaction and therefore transfers no energy to the medium, it does not seem to offer any possibilities for detection of the passage of the photon. For this reason, only the three common interactions are discussed in further detail below.

Also note that the reaction products of all three major processes consist solely of energetic electrons, and photons in the X-ray and gamma ray range. The more exotic processes lead to the production of neutrons, protons, and other particles. However, under even the most favorable conditions, the amount of energy converted into these other particles is a small fraction of the total.

Figure A-1 is a plot of the linear attenuation coefficient of germanium, showing not only the total, but also the relative contributions of each of the three major interaction processes.

Figure A-1. Gamma Ray Linear Attenuation Coefficient of Germanium

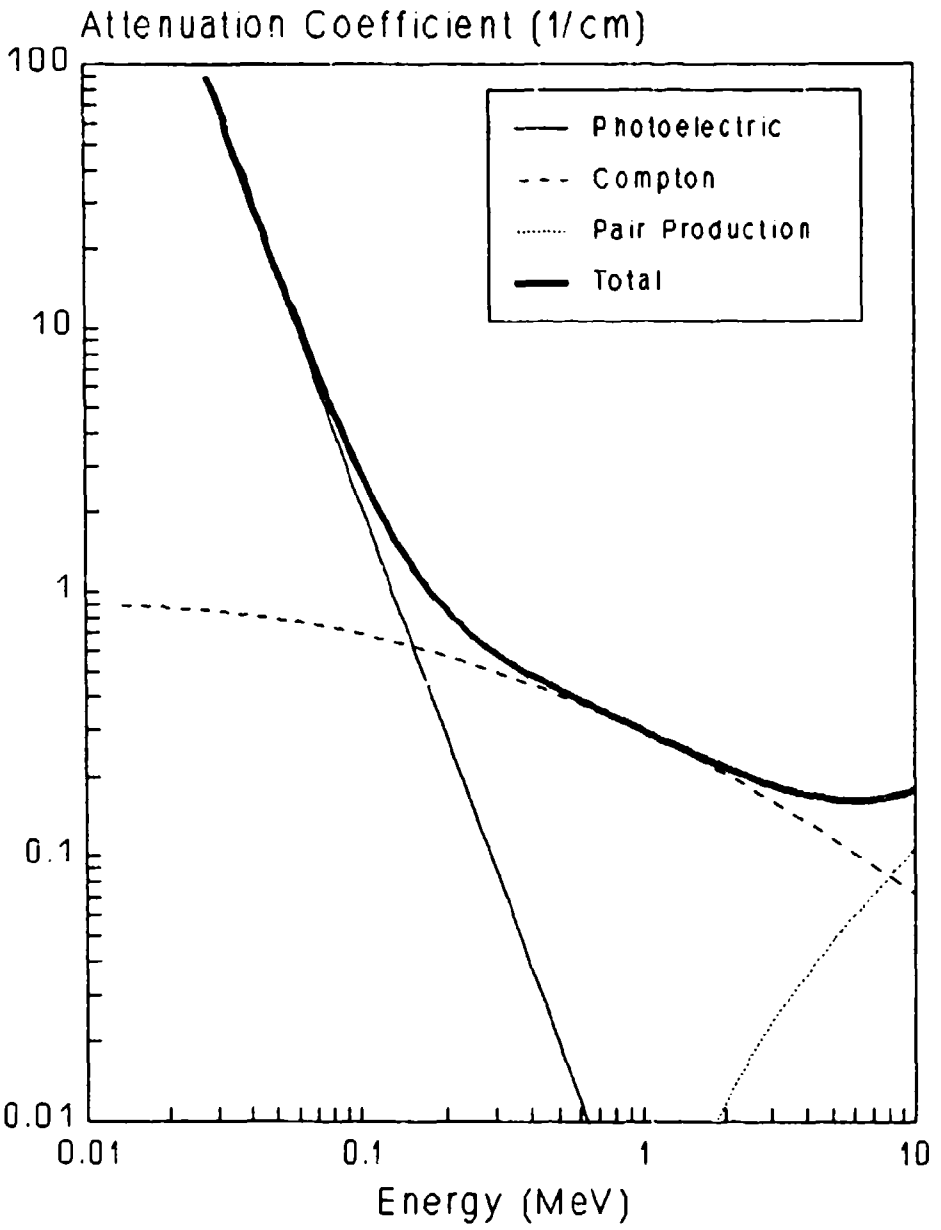

A.2. DESCRIPTION OF MAJOR PROCESSES

The three major photon interaction processes identified in Section A.1 are described more fully below.

A.2.1. Photoelectric Effect

One bound electron receives the entire photon energy and flies off with kinetic energy equal to the photon energy, minus the binding energy of the electron. No time lag between the beginning of irradiation and the appearance of photoelectrons has ever been measured, according to a search of recent literature.

For the photoelectric effect to occur, the electron must look "bound" to the photon. Therefore, the process is favored for atoms with high nuclear charge; the probability of the photoelectric effect is roughly proportional to Z^5 for energy > 0.1 MeV. The process is also favored by low gamma energy; the probability is roughly proportional to E^{-3} below 0.5 MeV, and roughly proportional to E^{-1} above 0.5 MeV.

The most strongly-bound electrons are those in the inner shells. Both theoretically and experimentally, it is found that ~80% of the photoelectric interactions are with K shell electrons. Most of the rest of the ionization is in the L shells. Since inner electrons are most affected, the ejection of the electron must be followed by the production of X-rays, as the ionized atom realigns itself.

The K shell energies of Ge are 9.8-11.1 keV. The L shell energies are 1.2-1.4 keV. Besides the fact that there is a range of K and L energies, ionization of the K shell does not necessarily lead to a K X-ray. The fluorescent yield of Ge is about 0.55, meaning that only about 55% of K shell ionizations lead to a K X-ray, and the rest produce a cascade of even lower-energy photons. These outer-shell X-rays would be absorbed in even less distance than the K X-rays.

All these X-rays have a very short range. Estimating the absorption coefficient for Ge to be ~220 cm^2/g at 10 keV, and taking the density of Ge to be 5.33 g/cm^3, the X-rays have a mean free path of ~8 μm, and are 99% absorbed in less than ~40 μm. The X-ray production may therefore be described as highly variable in energy per photon, with the total energy absorbed in the immediate vicinity of the interaction.

The ejected photoelectron carries all of the energy other than the small X-ray component. The path of the electron is predominately sidewards (relative to the photon direction) at low energy, and is more nearly aligned with the photon direction at higher energy. Specifically, the median direction ("bipartition angle") is -75° at 0.02 MeV, and -11° at 2.76 MeV. The range of a 2-MeV electron is -1 g/cm^2, which is equivalent to -2 mm in Ge.

It seems unlikely that current technology will support a means for resolving locations of energy deposition that could distinguish the 2 mm range of the electrons, much less the 40 μm range of the X-rays, inside a Ge detector a few cm in size. Therefore, the common characterization of the photoelectric effect as a "local" absorption process is accurate for practical detection purposes.

A.2.2. Compton Effect

One loosely-bound/unbound electron receives part of the energy of the photon, which is scattered through an angle that depends on the fraction of energy transferred. Maximum energy is transferred when the gamma is backscattered (i.e., scattered through 180°).

The probability of a Compton interaction is equal for each orbital electron. Therefore, the probability of a Compton event per atom of interacting medium is proportional to the number of orbital electrons; this is the same as saying that the Compton probability is proportional to Z of the absorber. The probability of Compton events is less energy-dependent than the photoelectric probability. At energies as high as 10 MeV, the Compton probability is still declining less rapidly than E^{-1}.

Since the Compton effect involves orbital electrons, it leads to the production of characteristic X-rays just as the photoelectric effect does. However, the Compton effect may involve any electron, not just a tightly-bound one. Therefore, the average X-ray energy in Compton interactions will be even less than in photoelectric interactions, and the X-ray energy will be deposited in an even smaller volume than the ~40 μm applicable to the photoelectric X-rays.

The Compton electron will also have lower energy than a photoelectron produced by the same incident photon, because the Compton electron receives less than the full energy of the photon. Therefore, the Compton electron energy will be deposited in an even smaller volume than the ~2 mm applicable to the 2-MeV photoelectrons.

The distinguishing mark of the Compton interaction is the occurrence of the scattered photon, which after leaving the site of the first interaction is subject to all three of the photon interaction processes. The scattered photon may have any energy between the incident energy and the minimum that occurs in the event of 180° backscatter. When the probability of a given scattering angle is folded in with the energy implied by that angle, the average fraction of the incident energy that is retained by the scattered photon can be computed. Over the energy range of interest, this average fraction of energy retained by the scattered gamma decreases from 0.861 for incident 0.1-MeV photons, to 0.423 for incident 3-MeV photons (Fa53).

Because of its appreciable energy, the scattered gamma will not necessarily be absorbed locally. For example, the minimum energy of the scattered gamma following the Compton interaction of a 0.1-MeV photon is ~70 keV. In Ge, 70-keV photons require ~0.7 cm for 99% absorption. As a second example, the maximum energy of the scattered gamma is the incident gamma energy. In Ge, 2-MeV photons require ~20 cm for 99% absorption, far larger than the practical thickness of a detector. Therefore, the interaction of the scattered gamma (if the scattered gamma interaction happens in the detector at all), may be at a location quite remote from that of the primary interaction. In fact, the higher the incident energy, the greater the distance between the first and second interaction sites.

The scattered photons are not emitted isotropically. Rather, there is a bias toward forward solid angles (minimum energy transfer) and toward backward solid angles (maximum energy transfer). As the incident photon energy increases, the bias toward forward solid angles becomes more pronounced. However, the 0° and 180° directions represent infinitesimal solid angles, so that no energy is scattered directly forward or directly backward.

Over the energy range of interest, the most probable direction of scattered photons shifts forward from about 50° (relative to the incident direction) for 0.05-MeV incident photons, to about 20° for 3-MeV incident photons. Because forward scatters represent higher retained energy, the preferred scattering direction of photon energy (as distinct from numbers of photons) is even more skewed toward the incident direction. However, the scattered photon energy is by no means monodirectional at any incident photon energy, as shown in the two parts of Figure A-2.

In summary, the characteristics of the scattered photons do not fall in a narrow and predictable band. The energy varies over a wide range, a range comparable to the range of incident energies. Although there is a preference for forward scattering of energy, the trend is not so pronounced that the sidewards and backwards contributions can be ignored without excluding a large number of events, especially at low incident energy. If the scattered photon interacts in the detector, that location could be within a fraction of a cm of the primary site (especially for low incident energy), but it may be anywhere in the detector (especially for high incident energy).

Figure A-2
Angular Distribution of Scattered Energy in Compton Interactions

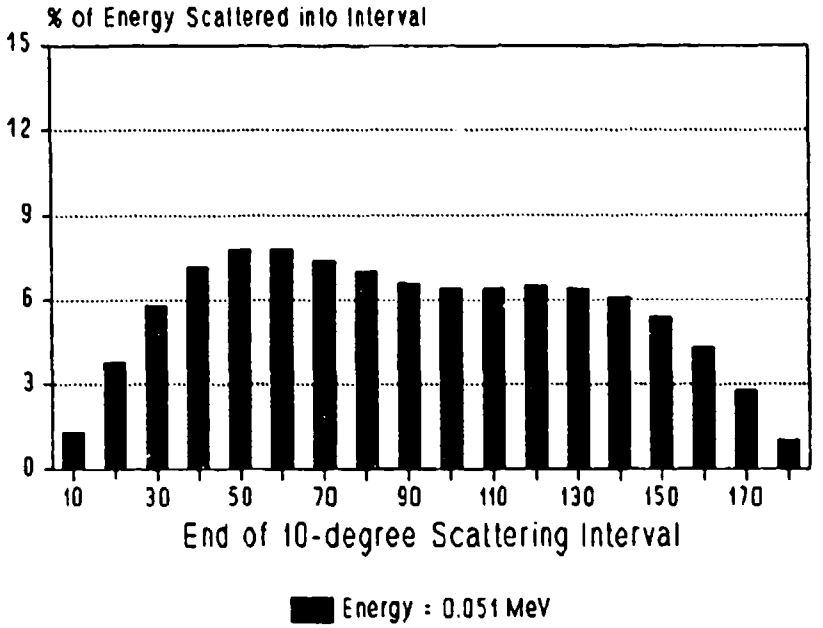

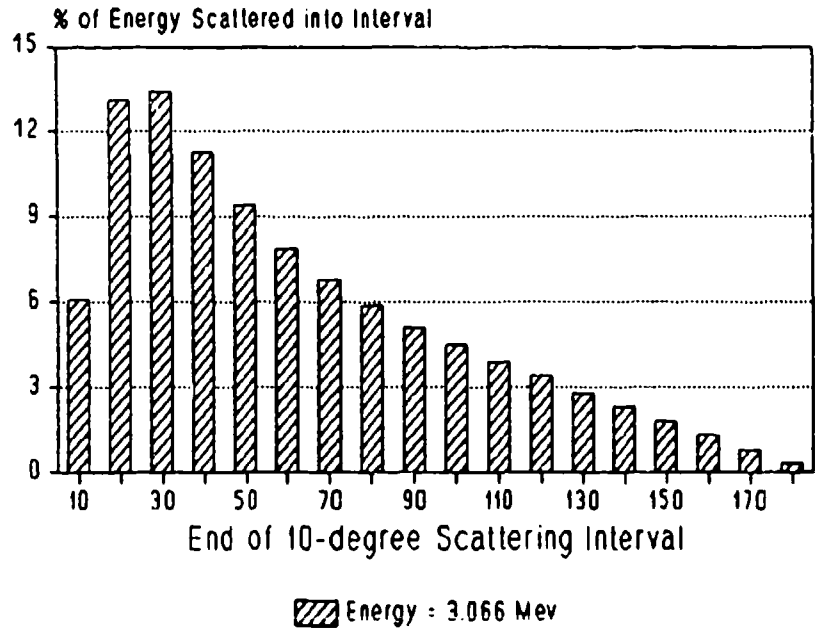

A.2.3. Pair Production Effect

In a pair production event, a photon reacts with an intense electromagnetic field, and is converted into one positive and one negative electron. At relatively low incident energies, all such reactions take place in the vicinity of a nucleus, but at higher energies orbital electrons may provide the electric field, and the pair may appear at a point comparatively remote from the nucleus.

Creating the mass of the two particles requires 1.02 MeV, which sets an absolute threshold for the reaction. The energy above the 1.02-MeV threshold goes into the kinetic energy of the electrons. The electrons surrender their kinetic energy to the medium by the normal ionization and excitation processes, and when the positron reaches thermal equilibrium with the medium, it is attracted to and annihilated by a negative electron. The annihilation produces two gamma rays, each of energy m_e (i.e., 0.511 MeV), which leave the annihilation site in approximately opposite directions (given that the momenta of the electrons at annihilation are equal and opposite). The annihilation photons are then subject to Compton interactions (but not pair production effects), until their ultimate disappearance in a photoelectric interaction.

Because of the opposite charges of the electrons, and the fact that the reaction takes place in the neighborhood of the positive nucleus, the positron has higher kinetic energy than the normal electron for low gamma energies, with the difference decreasing for increasing gamma energy. For example, in lead at 1.53-MeV gamma energy, the positron gets 0.42 MeV in kinetic energy, and the normal electron gets 0.09 MeV; at 2.66-MeV gamma energy, the breakdown is 1.10 MeV for the positron and 0.54 MeV for the normal electron (Da52). The initial direction of the electrons is predominately forward because of the high momentum of the incident gamma ray, but their subsequent scatters ultimately randomize their directions.

In view of their unextraordinary energies, the electron pair has no particularly distinguishing characteristics, other than that one of the electrons is positively charged. They may be expected to give up their kinetic energy in a few mm, like the electrons produced in all gamma interactions discussed above.

Since the pair production event itself does not involve displacement of orbital electrons, it does not lead directly to the production of characteristic X-rays as the photoelectric and Compton interactions do.

Absorption of the annihilation photons (if it occurs in the detector) will certainly lead to a wide dispersal of charge production. This is true on two grounds. First, the gammas have initial energy of 0.511 MeV each, for which the mean free path in Ge is ~2.2 cm and the distance for 99% absorption is ~10 cm. Second, their initial directions are 180° apart; considering their mean free paths, it is then very unlikely that their first interaction sites will be near each other.

It follows from the above discussion that (like Compton events and unlike photoelectric events) pair production events are likely to cause charge production over several cm^3 of the detector volume. The pattern of charge production is not simply related to the location of the pair production event, or to the incident photon energy or direction.

In principle, it should take longer for charge production to be completed in the pair production case than in the Compton case because of the production of two generations of electrons (the pair electrons and the post-annihilation Compton and photoelectrons). The electrons have sub-light speeds, and therefore require finite time to traverse the detector volume and lose their energy. However, the electron velocities are very high and the distances are fairly short. For example, a 2-MeV electron is a relativistic particle with a velocity of $0.98c$. If such an electron had an average velocity over its lifetime as low as $0.01c$, it would still traverse its 0.2 cm range in Ge in only 0.7 nsec. This is likely to be an insignificant contributor to a signal rise time that is overall no shorter than ~50 nsec.

A.3. REFERENCES

Da52 Davisson, C. M.; Evans, R. D. "Gamma-Ray Absorption Coefficients." Revs. Modern Phys. 24: 79-107; 1952.

Ev55 Evans, R. D. The Atomic Nucleus. New York: McGraw-Hill Book Co; 1955.

Fa53 Fano, U. "Gamma Ray Attenuation. Part I. Basic Processes." Nucleonics 11 (8): 8-12; 1953.

APPENDIX B

Description of Monte Carlo Model Used in the Present Research

It is important to understand that the development of gamma ray event sequences was completely separate from the study or evaluation of the sequences. That is, the process of evaluating potential event sequence discrimination methods had the following two steps:

1. For each gamma energy of interest, run the Monte Carlo model for a large number of gamma rays, and develop a list of the interaction sequences which occur in the detector volume.

2. For each event sequence discrimination method of interest, examine the event sequence files to determine what spectrum would result from the application of the method at energy of interest.

The two steps were separated because the first is much more computationally intensive, and did not need to be repeated for every conceivable different discrimination method: the same sequence files could simply be parsed using different criteria for accepting or rejecting a sequence for counting. In addition, given the same seed for the pseudo-random number generator which is at the heart of the Monte Carlo model, the exact same event sequences would always occur for a given source energy. This means that repeated running of the Monte Carlo model would not have been any more informative than was the method used.

Operationally, the results of the Monte Carlo model for each gamma energy were stored in a computer file with contents like those shown in Figure B-1. A separate event sequence list was recorded for each gamma ray interacting in the detector. For each interaction in each such sequence, the following were recorded: type of interaction, location of the interaction (distance from top of detector, and distance from axis of detector); and amount of energy deposited in the interaction. Note that these data are sufficient to support the application of any reasonable event sequence discrimination method that might be based on criteria such as the following: number of events in the sequence; type of events in the sequence; and/or location or distribution of locations of events in the sequence.

Figure B-1. Example All-Event Sequence Listing

Energy: 1836.00 keV Randomize Seed: 4567
Source to Detector Distance: 10.00 cm
Detector Thickness: 8.00 cm Radius: 3.00 cm

#:	Type	Dep. Energy	R	Z
1	Compton	1491.12 keV	2.20 cm	1.17 cm
	ESCAPE	0.00 keV	8.67 cm	10.89 cm
2	Compton	1310.22 keV	1.40 cm	3.18 cm
	Compton	300.15 keV	2.16 cm	3.41 cm
	Compton	27.63 keV	2.15 cm	3.46 cm
	ESCAPE	0.00 keV	4.37 cm	13.88 cm
3	Compton	1292.86 keV	2.04 cm	1.34 cm
	ESCAPE	0.00 keV	5.66 cm	12.15 cm
4	Pass Thru	0.00 keV	1.44 cm	18.01 cm
5	Compton	899.84 keV	2.28 cm	7.23 cm
	ESCAPE	0.00 keV	5.93 cm	20.31 cm
6	Pass Thru	0.00 keV	3.98 cm	14.24 cm
7	Pass Thru	0.00 keV	3.97 cm	13.92 cm
8	Compton	4.02 keV	1.23 cm	3.03 cm
	Compton	1482.84 keV	1.52 cm	5.72 cm
	Compton	190.76 keV	1.28 cm	5.68 cm
	Compton	55.18 keV	1.33 cm	5.77 cm
	Photo-Electric	103.19 keV	1.32 cm	5.75 cm
9	Compton	648.81 keV	2.87 cm	1.63 cm
	ESCAPE	0.00 keV	6.44 cm	15.10 cm
10	Compton	948.75 keV	2.34 cm	0.92 cm
	Compton	70.06 keV	2.35 cm	0.94 cm
	ESCAPE	0.00 keV	21.85 cm	18.87 cm
11	Compton	445.05 keV	2.63 cm	0.72 cm
	ESCAPE	0.00 keV	8.76 cm	23.81 cm

The following sections provide a description of the Monte Carlo model used for developing event sequences in HPGe gamma spectrometers. That is, they describe only the model used in the first of the two steps listed above. The event sequence discriminators used in the second step are discussed in Section 3.0.

The particular model used was based on a model from earlier work. However, the original model contained some generalities not relevant to the current research, and was implemented with computer hardware and software which are no longer available. For these reasons, a new implementation of the former model was developed, with features applicable to the current research, and using modern software and hardware. (Specifically, the code was written in the C language, and compiled under Microsoft C version 5.1. It was executed on a desk-top computer equipped with an 80386 processor and an 80387 math co-processor.)

The algorithms used for modelling the physical processes were not changed from the earlier work. Therefore, although the description below is intentionally abbreviated, the full discussion of the algorithms published previously is still applicable (Wa70a).

B.1. PRINCIPAL FEATURES

Geometry. The model handles point sources of activity, and bare solid cylindrical detector crystals. The source may be located at any desired distance from one of the flat faces of the detector, on the extended axis of the detector cylinder. The void space at the core of a closed-end coaxial detector, and scattering from external materials (cold finger, cryostat, mounting hardware, etc.) were considered second-order effects, and were not included in the model. Subsequent models used for detector design would need to include these second-order effects.

Energy Range. Monoenergetic gamma ray sources with an original energy in the range of 50 keV to 10 MeV may be specified. The energy restriction is not due to any inherent properties of the model, but rather is due to the following factors. First, the model uses simplified fitted forms of published interaction cross-section data, and the energies should be restricted to the range where the fits are acceptable. Second, on the low energy end, the shielding effects of detector packaging and dead layers, which are both outside the detector sensitive volume, are not modeled; therefore, the results for energies below 50-75 keV would be grossly unrealistic.

Interactions. Because of the energy range of interest, and the objective of modeling only those interactions which deposit energy in the crystal, only the three major gamma interactions (photoelectric, Compton, and pair production) are included in the model. The cross-section for each interaction as a function of energy is a mathematical fit to published data, and is not calculated from first physical principles. Pure germanium is assumed.

Calculational Steps. The basic logic flow of the Monte Carlo model code is illustrated in Figure B-2. The following narrative steps further explain the sequence:

1. Read in geometric and energy data. Based on geometry, calculate fraction of gamma rays which would not strike detector volume; save this number to correct for geometric effects.

2. If desired maximum number of emitted gammas has been processed, stop. Otherwise, select direction for new gamma ray, based on a random number. Since geometric effects already accounted for, restrict direction to one which would strike detector. Begin event sequence record. [Note: Until after the first interaction, gamma energy is original energy read in at step (1).]

3. Decide whether gamma interacts in crystal, and if so, where. Decision is based on total interaction cross-section at current energy, path length through crystal at the current direction, and a random number. If gamma passes out of detector without interacting, record the escape, end the event sequence, and return to step (2) for new gamma. Otherwise, continue.

4. Select type of interaction occurring. Selection is based on relative probabilities of the three interaction types at current energy, and a random number. Go to appropriate step, based on selected interaction: for photoelectric, step (5); for Compton, step (6); for pair production, step (7).

5. Complete the event sequence for the original gamma ray by recording the type, location, and energy deposited in the photoelectric event. Return to step (2) for new gamma.

6. Determine the direction of the scattered gamma ray, relative to the direction of the gamma experiencing the Compton interaction, based on the tabulated Klein-Nishina probabilities and one random number. From the selected scattering angle compute the energy deposited, and record the type, location, and energy deposited in the Compton

event. Determine the other component of the scattered gamma direction based on another random number. Return to step (3) and continue processing scattered gamma until it is either totally absorbed or a scattered gamma escapes the crystal.

7. Record the pair production event's location and energy deposited (= current energy - 1.02 MeV). Using two random numbers, select a direction for the first annihilation gamma. Given its energy (511 keV), process it through steps similar to (3)-(6) above, except that when its sequence is complete, process the other annihilation gamma as follows. [Note: The annihilation gammas cannot themselves experience pair production.]

Assign the second annihilation gamma to the direction diametrically opposite to that assigned to the first. Given its energy (511 keV), process it through steps similar to (3)-(6) above. When its sequence is complete, end the entire event sequence record of the original emitted gamma ray, and return to step (2) for a new gamma.

Figure B-2. Simplified Logic Flow of Monte Carlo Code

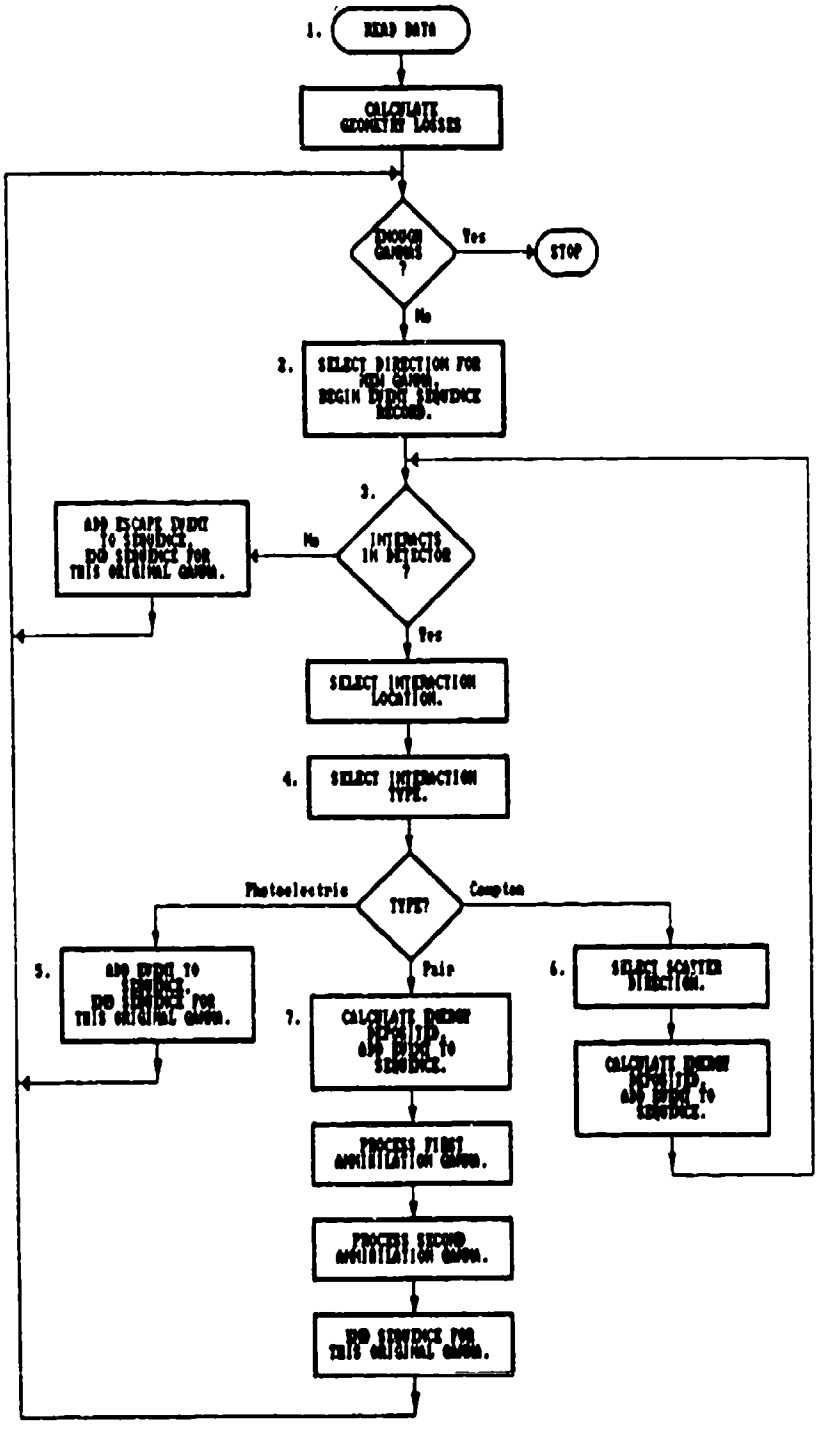

B.2. EFFECTS NOT INCLUDED

Complete description of the Monte Carlo model used requires acknowledgment of several effects which it does not include. The most important of these effects are listed below, with an assessment of the likely impact of their exclusion from the model.

Azimuthal Location. As shown in the example sequence listing of Figure B-1, only two coordinates are recorded for each interaction in a sequence: the depth into the crystal, and the distance from the central axis. The initial gamma is not assigned an angle around the central axis, so no azimuthal coordinate can be computed for any interaction location.

Because of the axial symmetry of the assumed cylindrical crystal, and the isotropic emissions of the source, events will be distributed evenly around the crystal axis. Therefore, no event sequence discriminators based on azimuthal event distributions are likely to be effective. In addition, the axial symmetry means that the azimuthal location of an interaction site is irrelevant for parameters such as in-detector pathlengths, so there is no need to track the azimuthal coordinate.

Electron Transport. Any electron produced by gamma interactions is assumed to deposit its energy locally at the point where it is created. In fact (see Appendix A), the electron's true range may be up to ~1 mm in germanium, depending on energy. This means that in a real detector the energy deposited would be somewhat more dispersed than is indicated by the model. It suggests that any event sequence discriminators based on location discrimination finer than a few mm are likely to have true performance which is less satisfactory than the theoretical performance inferred from the Monte Carlo model runs.

X-ray Escapes. All X-ray production and transport is ignored, whether the X-rays would arise from Bremsstrahlung losses from energetic electrons, or from radiative de-excitation of germanium atoms in the crystal lattice. (This is related to the electron transport effect just discussed.) The range of such X-rays would be in the tens of μm (see Appendix A), so their energy would be deposited even more locally than would that of electrons.

The larger the detector crystal, the less likely it becomes that these X-rays would escape partially or totally. For example, in a 5 cm diameter by 5 cm thick cylinder, the outer 50 μm (where the X-ray has at least some chance to escape) contains only 0.6% of the total cylinder volume.

Nevertheless, very small germanium escape peaks are sometimes seen about 11 keV below very intense peaks in real spectra. Such peaks will not be seen in the spectra based on the results of this Monte Carlo model.

Background. The model does not attempt to simulate the effects of background counts caused by either cosmic rays or terrestrial radionuclides. These background components are highly dependent on the application, and cannot be meaningfully included in a general model. As a result, the spectra produced do not show the expected rise toward the low-energy end, as well as both the peak and Compton contributions of natural nuclides. All these effects worsen the sensitivity of real spectrometers at low energy. For any specific application, the background components could be included and modeled as desired.

Attenuation Between Source and Detector Crystal. No materials outside the sensitive volume of the detector are included in the model. The most important of these materials are the dead layer, mounting hardware, and cryostat end cap, all of which tend to attenuate low-energy gammas before they reach the sensitive volume, and which therefore lower the efficiency. The degree of this attenuation is independent of the methods (if any) used for event sequence discrimination. Therefore, the non-modeling of this effect does not affect the comparison between methods, which is all that is attempted in this research.

B.3. REFERENCES

Wa70a Walker, D.M. "An Investigation of Multiple Gamma Scattering in Germanium as Applied to Ge(Li) Gamma Spectrometers." Atlanta, GA: Georgia Institute of Technology; Thesis; 1970.